



**HAL**  
open science

## Triangulating submanifolds: An elementary and quantified version of Whitney's method

Jean-Daniel Boissonnat, Siargey Kachanovich, Mathijs Wintraecken

### ► To cite this version:

Jean-Daniel Boissonnat, Siargey Kachanovich, Mathijs Wintraecken. Triangulating submanifolds: An elementary and quantified version of Whitney's method. 2018. hal-01950149v1

**HAL Id: hal-01950149**

**<https://inria.hal.science/hal-01950149v1>**

Preprint submitted on 10 Dec 2018 (v1), last revised 12 May 2023 (v2)

**HAL** is a multi-disciplinary open access archive for the deposit and dissemination of scientific research documents, whether they are published or not. The documents may come from teaching and research institutions in France or abroad, or from public or private research centers.

L'archive ouverte pluridisciplinaire **HAL**, est destinée au dépôt et à la diffusion de documents scientifiques de niveau recherche, publiés ou non, émanant des établissements d'enseignement et de recherche français ou étrangers, des laboratoires publics ou privés.

# Triangulating submanifolds: An elementary and quantified version of Whitney’s method

**Jean-Daniel Boissonnat**

Université Côte d’Azur, INRIA  
[Sophia-Antipolis, France]  
jean-daniel.boissonnat@inria.fr

**Siargey Kachanovich**

Université Côte d’Azur, INRIA  
[Sophia-Antipolis, France]  
siargey.kachanovich@inria.fr

**Mathijs Wintraecken**

Université Côte d’Azur, INRIA  
[Sophia-Antipolis, France]  
m.h.m.j.wintraecken@gmail.com

## 1 — Abstract —

2 We quantize Whitney’s construction to prove the existence of a triangulation for any  $C^2$  manifold,  
3 so that we get an algorithm with explicit bounds. We also give a new elementary proof, which is  
4 completely geometric.

**2012 ACM Subject Classification** Theory of computation → Computational geometry

**Keywords and phrases** Triangulations, Manifolds, Coxeter triangulations

**Related Version** A full version of this paper is available at <https://hal.inria.fr/hal-?????>  
??

**Funding** This work has been partially funded by the European Research Council under the European Union’s ERC Grant Agreement number 339025 GUDHI (Algorithmic Foundations of Geometric Understanding in Higher Dimensions).

**Lines** 483

## 5 **1** Introduction

6 The question whether every  $C^1$  manifold admits a triangulation was of great importance to  
7 topologists in the first half of the 20th century. This question was answered in the affirmative  
8 by Cairns [11], see also Whitehead [26]. However the first proofs were complicated and not  
9 very geometric, let alone algorithmic. It was Whitney [27, Chapter IV], who eventually gave  
10 an insightful geometric constructive proof. Here, we will be reproving Theorem 12A of [27,  
11 Section IV.12], in a more quantitative/algorithmic fashion for  $C^2$  manifolds:

12 ► **Theorem 1.** *Every compact  $n$ -dimensional  $C^2$  manifold  $\mathcal{M}$  embedded in  $\mathbb{R}^d$  with reach*  
13  *$\text{rch}(\mathcal{M})$  admits a triangulation.*

14 By more quantitative, we mean that instead of being satisfied with the existence of constants  
15 that are used in the construction, we want to provide explicit bounds in terms of the reach  
16 of the manifold, which we shall assume to be positive. The reach was introduced by Federer  
17 [19], as the minimal distance between a set  $\mathcal{M}$  and its medial axis. The medial axis consists



© Jean-Daniel Boissonnat, Siargey Kachanovich, and Mathijs Wintraecken;  
licensed under Creative Commons License CC-BY

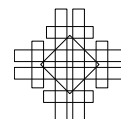
35th International Symposium on Computational Geometry (SoCG 2019).

Editors: Gill Barequet and Yusu Wang; Article No. 00; pp. 00:1–00:32

Leibniz International Proceedings in Informatics



LIPIC Schloss Dagstuhl – Leibniz-Zentrum für Informatik, Dagstuhl Publishing, Germany



18 of points in ambient space that do not have a unique closest point on  $\mathcal{M}$ . It is not too  
 19 difficult to generalize the precise quantities to the setting where the manifold is  $C^{1,1}$  at a  
 20 small cost, see Appendix B.

21 Note that Theorem 1 implies that any  $C^1$  manifold admits a triangulation. This is  
 22 because any  $C^1$  manifold can be smoothed (see for example [20]) and Whitney’s own em-  
 23 bedding theorem (see [27, Section IV.1]) gives an embedding in  $\mathbb{R}^d$ .

24 Triangulations in computational geometry/topology are most often based on Voronoi/Delaunay  
 25 triangulations of the input point set, see for example [3, 4, 9, 12, 15]. Whitney’s  
 26 construction is of a quite different nature. He uses an ambient triangulation and construct  
 27 the triangulation of the manifold  $\mathcal{M}$  based on the intersections of  $\mathcal{M}$  with this triangu-  
 28 lation. In this paper, we have chosen this ambient triangulation  $\tilde{\mathcal{T}}$  to be (a perturbation  
 29 of) a Coxeter triangulation  $\mathcal{T}$  of type  $\tilde{A}_d$ . A Coxeter triangulation of type  $\tilde{A}_d$  is Delaunay  
 30 protected, a concept we’ll recall in detail in Section 4. Delaunay protection gives that the  
 31 triangulation is stable under perturbations. This property simplifies the proof, which in fact  
 32 was one of the motivations for our choice. Moreover, Coxeter triangulations can be stored  
 33 very compactly, in contrast with previous work [9, 12] on Delaunay triangulations.

34 The approach of the proof of correctness of the method, that we present in this paper,  
 35 focuses on proving that after perturbing the ambient triangulation the intersection of each  $d$ -  
 36 simplex in the triangulation  $\tilde{\mathcal{T}}$  with  $\mathcal{M}$  is a slightly deformed  $n$ -dimensional convex polytope.  
 37 The triangulation  $K$  of  $\mathcal{M}$  consists of a barycentric subdivision of a straightened version of  
 38 these polytopes. This may remind the reader of the general result on CW-complexes, see  
 39 [21], which was exploited by Edelsbrunner and Shah [18] for their triangulation result. This  
 40 interpretation of Whitney’s triangulation method is different from the Whitney’s original  
 41 proof where the homeomorphism is given by the closest point projection and uses techniques  
 42 which we also exploited in [8]. Here we construct ‘normals’ and a tubular neighbourhood  
 43 for  $K$  that is compatible with the ambient triangulation  $\tilde{\mathcal{T}}$  and prove that the projection  
 44 along these ‘normals’ is a homeomorphism. We believe that the tubular neighbourhood we  
 45 construct is of independent interest. Because we have a bound on the size of the tubular  
 46 neighbourhood of  $K$  and  $\mathcal{M}$  lies in this neighbourhood, we automatically bound the Haus-  
 47 dorff distance between the two. A bound on the difference between the normals of  $K$  and  
 48  $\mathcal{M}$  is also provided. Thanks to our choice of ambient triangulation and our homeomorphism  
 49 proof, this entire paper is elementary in the sense that no topological results are needed, all  
 50 arguments are geometrical.

51 In addition to the more quantitative/algorithmic approach, the purely geometrical homeo-  
 52 morphism proof, the link with the closed ball property, the tubular neighbourhood for the  
 53 triangulation  $K$ , and a bound on the Hausdorff distance, we also give different proofs for a  
 54 fair number of Whitney’s intermediate results.

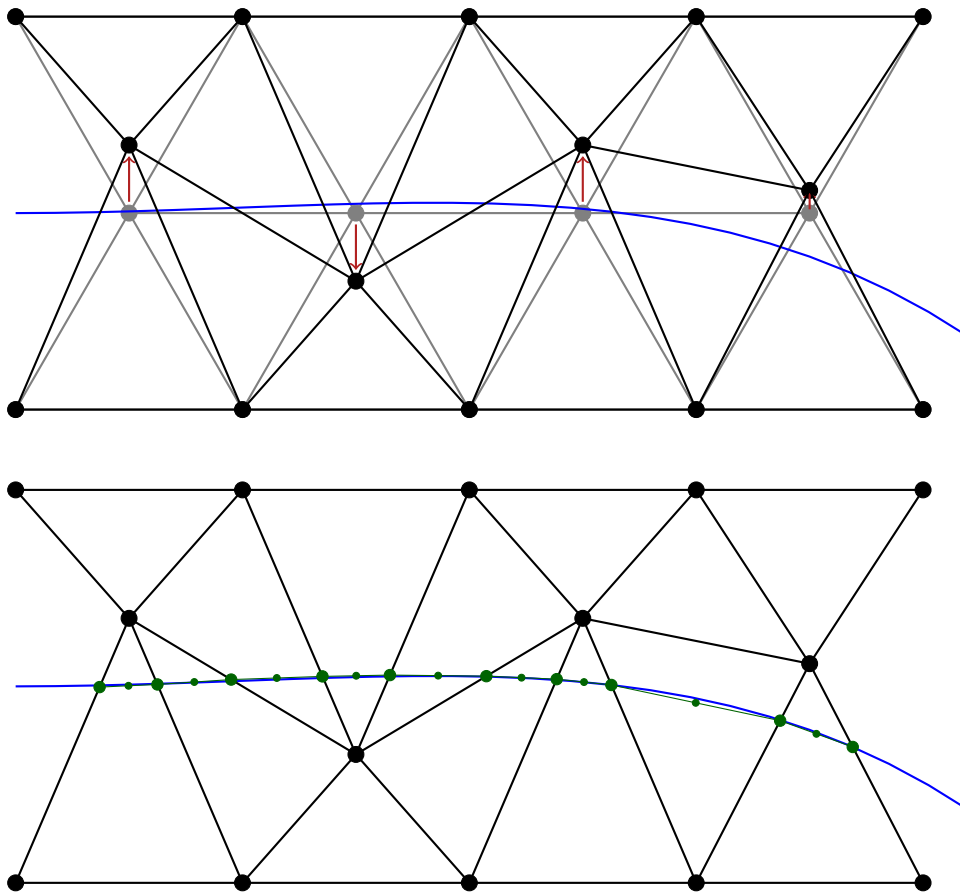
55 The algorithm described in this paper is being implemented at the moment. The results  
 56 will be reported in a companion paper.

57 All proofs of statements that are not recalled from other papers are given in the appendix.

## 58 **2 The algorithm and overview**

### 59 **2.1 The algorithm**

60 The algorithm takes as input an  $n$ -dimensional  $C^2$  manifold  $\mathcal{M} \subset \mathbb{R}^d$  with reach  $\text{rch}(\mathcal{M})$ ,  
 61 and outputs the triangulation  $K$  of  $\mathcal{M}$ . The algorithm based on Whitney’s construction  
 62 consists of two parts.



63 **Figure 1** The two parts of the algorithm: Part 1, where we perturb the vertices of the ambient  
 64 triangulation, is depicted on top. Part 2, where the triangulation is constructed from the points of  
 65 intersection of  $\mathcal{M}$  and the edges, is depicted below.

66 **Part 1.** This part of the algorithm handles the ambient triangulation and consists of  
 67 the following steps:

- 68 ■ Choose a Coxeter triangulation  $\mathcal{T}$  of type  $\tilde{A}_d$  of  $\mathbb{R}^d$  that is sufficiently fine (as determined  
 69 by the longest edge length  $L$ , see (8)).
- 70 ■ Perturb the vertices of  $\mathcal{T}$  slightly (see (14)) into a  $\tilde{\mathcal{T}}$  (with the same combinatorial  
 71 structure), such that all simplices in  $\tilde{\mathcal{T}}$  of dimension at most  $d - n - 1$  are sufficiently  
 72 far away from the manifold, see (11). This is done as follows: One maintains a list of  
 73 vertices and simplices of  $\tilde{\mathcal{T}}_i$ , starting with an empty list and adding perturbed vertices,  
 74 keeping the combinatorial structure of  $\mathcal{T}$  intact. This means that if  $\tau = \{v_{j_1}, \dots, v_{j_k}\}$   
 75 is a simplex in  $\mathcal{T}$  and  $\tilde{v}_{j_1}, \dots, \tilde{v}_{j_k} \in \tilde{\mathcal{T}}_i$ , where  $\tilde{v}_i$  denotes the perturbed vertex  $v_i$ , then  
 76  $\tilde{\tau} = \{\tilde{v}_{j_1}, \dots, \tilde{v}_{j_k}\}$  is a simplex in  $\tilde{\mathcal{T}}_i$ . To this list, one first adds all vertices of  $\mathcal{T}$  that are  
 77 very far from  $\mathcal{M}$ , as well as the simplices with these vertices (see Case 1 of Section 5.2).  
 78 For a vertex  $v_i$  that is relatively close to  $\mathcal{M}$  (Case 2), one goes through the following  
 79 procedure. We first pick a point  $p \in \mathcal{M}$  that is not too far from  $v_i$ . We then consider  
 80 all  $\tau'_j \subset \tilde{\mathcal{T}}_{i-1}$  of dimension at most  $d - n - 2$ , such that the join  $v_i * \tau'_j$  lies in  $\tilde{\mathcal{T}}_i$ . For all  
 81 such  $\tau'_j$  we consider  $\text{span}(\tau'_j, T_p \mathcal{M})$  and we pick our perturbed  $v_i$ , that is  $\tilde{v}_i$ , such that it  
 82 lies sufficiently far from the union of these spans (see (27)).

83 Note that we only require limited knowledge of the manifold. Given a vertex  $v_i$  we need  
 84 to be able to find a point on  $\mathcal{M}$  that is close to  $v_i$  or know if  $v_i$  is far from  $\mathcal{M}$  and we  
 85 need access to  $T\mathcal{M}$  in a finite sufficiently dense set of points (so that for every point  $v_i$  that  
 86 is close to  $\mathcal{M}$  we have a linear approximation of  $\mathcal{M}$ ). We assume we have two oracles for  
 87 the two operations. There are no fundamental difficulties in including small uncertainties  
 88 in our knowledge of the close points or the tangent spaces, but the analysis would be more  
 89 complicated. If we can sample  $\mathcal{M}$  densely finding close points is algorithmically not difficult.  
 90 Methods to estimate the tangent space have been described in [1].

91 **Complexity of part 1.** The complexity of the perturbation (per vertex) of the al-  
 92 gorithm is dominated by the number of simplices  $\tau'_j$  that we have to consider. This number  
 93 is bounded by the number of simplices of at most dimension  $d - n - 2$  in the star of a  
 94 vertex in a Coxeter triangulation plus 1, see (3) below. The number of simplices in turn is  
 95 bounded by  $(d - n)^d d^{(d-n)}$ , see claim 15. This compares favourably with the complexity  
 96 of the perturbation method in [5] for Delaunay triangulations, which is of order  $\mathcal{O}(2^{d^2})$ .  
 97 A full analysis of the complexity of the algorithm, including basic operations on Coxeter  
 98 triangulations, will be reported upon in a separate paper.

99 **Part 2.** The construction of the triangulation of  $\mathcal{M}$  is now straightforward barycentric  
 100 subdivision, for each  $\tau^k \in \tilde{\mathcal{T}}$ , of dimension  $k$  that contains a part of  $\mathcal{M}$ , we pick a point  
 101  $v(\tau^k)$  in  $\tau^k$ , see (19). For any sequence  $\tau^{d-n} \subset \tau^{d-n+1} \subset \dots \subset \tau^d$ , such that all simplices  
 102 in the sequence contain a part of  $\mathcal{M}$  we add a simplex  $\{v(\tau^{d-n}), \dots, v(\tau^d)\}$  to a simplicial  
 103 complex  $K$ . If we have done this for all simplices that contain  $\mathcal{M}$ ,  $K$  is a triangulation of  
 104  $\mathcal{M}$ .

105 For this second part we need an oracle that is able to tell us if the intersection between  
 106  $\mathcal{M}$  and  $\tau^{d-n} \in \tilde{\mathcal{T}}$  is non-empty and if so, gives us the point of intersection. As we'll see in  
 107 Section 6.1, it would in fact suffice to be able to find intersections between tangent planes  
 108 and simplices.

## 109 2.2 Outline and overview of the proof

110 This paper is dedicated to the correctness proof of the algorithm presented above. After some  
 111 background sections dedicated to manifolds of positive reach and Coxeter triangulations and  
 112 their stability under perturbations, we continue with the perturbation algorithm.

113 **The ambient triangulation.** In Section 5, we both give the details of the perturbation  
 114 of the vertices.

115 **The triangulation of  $\mathcal{M}$ .** In Section 6, the triangulation  $K$  of  $\mathcal{M}$  is defined and an  
 116 important quality bound for the simplices is given.

117 **The triangulation proof.** Section 7 is dedicated to proving that  $K$  is a triangulation of  
 118  $\mathcal{M}$ . The proof is quite different from the approach Whitney described, which uses the closest  
 119 point projection onto  $\mathcal{M}$ . Here we construct a tubular neighbourhood and 'normals' around  
 120 the triangulation  $K$ , which is adapted to the ambient triangulation  $\tilde{\mathcal{T}}$ . We then prove that  
 121 the projection using these 'normals' gives a piecewise smooth homeomorphism from  $\tau^d \cap \mathcal{M}$   
 122 to  $\tau^d \cap K$ , where  $\tau^d \in \tilde{\mathcal{T}}$  is  $d$ -dimensional. Because the construction is compatible on the  
 123 faces of  $d$  dimensional simplices the global result immediately follows. A more detailed  
 124 overview of the homeomorphism proof is given in Section 7.

## 125 3 Manifolds, tangent spaces, distances and angles

126 In this section, we discuss some general results that will be of use. The manifold  $\mathcal{M} \subset \mathbb{R}^d$   
 127 is a compact  $C^2$  manifold with reach  $\text{rch}(\mathcal{M})$ .

128 We adhere as much as possible to the same notation as used in [10]. The tangent bundle  
 129 will be denoted by  $T\mathcal{M}$ , while the tangent space at a point  $p$  is written as  $T_p\mathcal{M}$ . Similarly,  
 130  $N\mathcal{M}$  is the normal bundle and  $N_p\mathcal{M}$  a normal space. Distances on the manifold will be  
 131 indicated by  $d_{\mathcal{M}}(\cdot, \cdot)$ , while we write  $d(\cdot, \cdot)$  for distances in the ambient Euclidean space, and  
 132  $|\cdot|$  for the length of vectors. A ball centred at  $x$  with radius  $r$  is denoted by  $B(x, r)$ .

133 The closest point projection of point  $x$  in the ambient space, such that  $d(x, \mathcal{M}) <$   
 134  $\text{rch}(\mathcal{M})$ , onto  $\mathcal{M}$  is denoted by  $\pi_{\mathcal{M}}(x)$ . The orthogonal projection onto the tangent  $T_p\mathcal{M}$  is  
 135 denoted by  $\pi_{T_p\mathcal{M}}(x)$ .

136 We will use a result from [10], which improves upon previous works such as Niyogi, Smale  
 137 and Weinberger [23]:

138 ► **Lemma 2** (Lemma 6 and Corollary 3 of [10]). *Suppose that  $\mathcal{M}$  is  $C^2$  and let  $p, q \in \mathcal{M}$ ,  
 139 then*

$$140 \quad \angle(T_p\mathcal{M}, T_q\mathcal{M}) \leq \frac{d_{\mathcal{M}}(p, q)}{\text{rch}(\mathcal{M})} \quad \text{and} \quad \sin\left(\frac{\angle(T_p\mathcal{M}, T_q\mathcal{M})}{2}\right) \leq \frac{|p - q|}{2\text{rch}(\mathcal{M})}.$$

141 We now prove that the projection onto the tangent space is a diffeomorphism in a neigh-  
 142 bourhood of size the reach of the manifold. This improves upon previous results by Niyogi,  
 143 Smale, and Weinberger [23] in terms of the size of the neighbourhood, and is a more quant-  
 144 itative version of results by Whitney [27].

145 We first recall some notation. Similarly to [10], we let  $C(T_p\mathcal{M}, r_1, r_2)$  denote the ‘filled  
 146 cylinder’ given by all points that project orthogonally onto a ball of radius  $r_1$  in  $T_p\mathcal{M}$  and  
 147 whose distance to this ball is at most  $r_2$ . We write  $\mathring{C}(T_p\mathcal{M}, r_1, r_2)$  for the open cylinder.  
 148 We now have:

149 ► **Lemma 3.** *Suppose that  $\mathcal{M}$  is  $C^2$  and  $p \in \mathcal{M}$ , then for all  $r < \text{rch}(\mathcal{M})$ , the projection  
 150  $\pi_{T_p\mathcal{M}}$  onto the tangent space  $T_p\mathcal{M}$ , restricted to  $\mathcal{M} \cap \mathring{C}(T_p\mathcal{M}, r, \text{rch}(\mathcal{M}))$  is a diffeomorphism  
 151 onto the open ball  $B_{T_p\mathcal{M}}(r)$  of radius  $r$  in  $T_p\mathcal{M}$ .*

152 It is clear by considering the sphere that this result is tight. See Appendix B for some  
 153 remarks on these results in the  $C^{1,1}$  setting.

154 ► **Definition 4.** We shall write  $\pi_p$  as an abbreviation for the restriction (of the domain) of  
 155  $\pi_{T_p\mathcal{M}}$  to  $\mathcal{M} \cap \mathring{C}(T_p\mathcal{M}, \text{rch}(\mathcal{M}), \text{rch}(\mathcal{M}))$  and  $\pi_p^{-1}$  for its inverse.

156 We now also immediately have a quantitative version of Lemma IV.8a of [27]:

157 ► **Lemma 5.** *Suppose that  $\mathcal{M}$  is  $C^2$ , then for all  $r < \text{rch}(\mathcal{M})$*

$$158 \quad d(p, \mathcal{M} \setminus C(T_p\mathcal{M}, r, \text{rch}(\mathcal{M}))) = d(p, \mathcal{M} \setminus \pi_p^{-1}(B_{T_p\mathcal{M}}(r))) \geq r. \quad (1)$$

159 We shall also need the following bound on the (local) distance between a tangent space  
 160 and the manifold.

161 ► **Lemma 6** (Distance to Manifold, Lemma 11 of [10]). *Let  $\mathcal{M}$  be a manifold of positive reach.  
 162 Suppose that  $w \in T_p\mathcal{M}$  and  $|w - p| < \text{rch}(\mathcal{M})$ . Let  $\pi_p^{-1}(w)$  be as in Definition 4. Then*

$$163 \quad |\pi_p^{-1}(w) - w| \leq \left(1 - \sqrt{1 - \left(\frac{|w - p|}{\text{rch}(\mathcal{M})}\right)^2}\right) \text{rch}(\mathcal{M}).$$

164 This is attained for the sphere of radius  $\text{rch}(\mathcal{M})$ .

165 **4 Coxeter triangulations, Delaunay protection and stability**

166 Coxeter triangulations [14] of Euclidean space play a significant role in our work. They  
 167 combine many of the advantages of cubes, with the advantages of triangulations. They are  
 168 also attractive from the geometrical perspective, because they provide simplices with very  
 169 good quality and some particular Coxeter triangulations are Delaunay protected and thus  
 170 very stable Delaunay triangulations. We will now very briefly introduce both the concepts  
 171 of Coxeter triangulations and Delaunay protection, but refer to [13] for more details on  
 172 Coxeter triangulations and to [5, 6] for Delaunay protection.

174 ► **Definition 7.** A monohedral<sup>1</sup> triangulation is called a *Coxeter triangulation* if all its  
 175  $d$ -simplices can be obtained by consecutive orthogonal reflections through facets of the  $d$ -  
 176 simplices in the triangulation.

177 This definition imposes very strong constraints on the geometry of the simplices, implying  
 178 that there are only a small number of such triangulations in each dimension. Most of  
 179 these triangulations are part of 4 families for which there is one member for (almost) every  
 180 dimension  $d$ . We will focus on one such family,  $\tilde{A}_d$ , which is Delaunay protected.

181 **Protection.**

182 ► **Definition 8.** The *protection* of a  $d$ -simplex  $\sigma$  in a Delaunay triangulation on a point set  
 183  $P$  is the minimal distance of points in  $P \setminus \sigma$  to the circumscribed ball of  $\sigma$ :

$$184 \quad \delta(\sigma) = \inf_{p \in P \setminus \sigma} d(p, B(\sigma)), \text{ where } B(\sigma) \text{ is the circumscribed ball of } \sigma.$$

185 The *protection*  $\delta$  of a Delaunay triangulation  $\mathcal{T}$  is the infimum over the  $d$ -simplices of the  
 186 triangulation:  $\delta = \inf_{\sigma \in \mathcal{T}} \delta(\sigma)$ . A triangulation with a positive protection is called *protected*.

187 The proof that  $\tilde{A}_d$  triangulations are protected can be found in [13, Section 6]. We shall  
 188 denote the triangulation of this type by  $\mathcal{T}$ .

189 **Stability.** In the triangulation proof below we need that a perturbation  $\tilde{\mathcal{T}}$  of our initial  
 190 ambient triangulation ( $\mathcal{T}$  of type  $\tilde{A}_d$ ) is still a triangulation of  $\mathbb{R}^d$ . Because Whitney did  
 191 not use a protected Delaunay triangulation he needs a non-trivial topological argument to  
 192 establish this, see [27, Appendix Section II.16]. The argument for stability of triangulations  
 193 for  $\tilde{A}$  type Coxeter triangulations is much simpler, because it is a Delaunay triangulation and  
 194  $\delta$ -protected, see [13]. Before we can recall this result we need to introduce some notation:

- 195 ■ The minimal altitude or height, denoted by  $\min \text{alt}$ , is the minimum over all vertices of  
 196 the altitude, that is the distance from a vertex to the affine hull of the opposite face.  
 197  $t(\tau)$  denotes the thickness of a simplex  $\tau$ , that is the ratio of the minimal altitude to the  
 198 maximal edge length. We write  $t(\mathcal{T})$  for thickness of any simplex in  $\mathcal{T}$ .
- 199 ■ We can think of the vertices of  $\mathcal{T}$  as an  $(\epsilon, \mu)$ -net. Here  $\mu$  is the separation (for Coxeter  
 200 triangulations, the shortest edge length in  $\mathcal{T}$ ), and  $\epsilon$  the sampling density (which is  
 201 the circumradius of the simplices in the Coxeter triangulation). We write  $\mu_0$  for the  
 202 normalized separation, that is  $\mu = \mu_0 \epsilon$ .
- 203 ■ For any complex  $K$ ,  $L(K)$  denotes the longest edge length in  $K$ . We use the abbreviations  
 204  $L = L(\mathcal{T})$  and  $\tilde{L} = L(\tilde{\mathcal{T}})$ .

205 Theorem 4.14 of [5] immediately gives:

---

173 <sup>1</sup> A triangulation of  $\mathbb{R}^d$  is called *monohedral* if all its  $d$ -simplices are congruent.

206 ► **Corollary 9.** *The triangulation  $\mathcal{T}$  is (combinatorially) stable under a  $\tilde{c}L$ -perturbation,*  
 207 *meaning that  $d(v_i - \tilde{v}_i) \leq \tilde{c}L$ , as long as*

$$208 \quad \tilde{c}L \leq \frac{t(\mathcal{T})\mu_0}{18d} \delta. \tag{2}$$

209 We claim the following concerning the behaviour of  $\tilde{c}$

► **Claim 10.**

$$210 \quad \tilde{c} \leq \frac{t(\sigma)\mu_0}{18d} \frac{\delta}{L} \leq \sqrt{2} \frac{\sqrt{d^2 + 2d + 24} - \sqrt{d^2 + 2d}}{9d^{3/2}\sqrt{d+2}(d+1)} \sim \frac{\sqrt{32}}{3d^4},$$

211 **Thickness and angles.** The quality of simplices and the control over the alignment of  
 212 the simplices with the manifold is an essential part of the triangulation proof, for which we  
 213 need two basic results. Similar statements can be found in Section IV.14 and Section IV.15  
 214 of [27].

215 We remind ourselves of the following:

216 ► **Lemma 11** (Thickness under distortion [17, Lemma 7]). *Suppose that  $\sigma = \{v_0, \dots, v_k\}$  and*  
 217  *$\tilde{\sigma} = \{\tilde{v}_0, \dots, \tilde{v}_k\}$  are two  $k$ -simplices in  $\mathbb{R}^d$  such that  $\|v_i - v_j| - |\tilde{v}_i - \tilde{v}_j|\| \leq c_0L(\sigma)$  for all*  
 218  *$0 \leq i < j \leq k$ . If  $c_0 \leq \frac{t(\sigma)^2}{4}$ , then  $t(\tilde{\sigma}) \geq \frac{4}{5\sqrt{k}}(1 - \frac{4c_0}{t(\sigma)^2})t(\sigma)$ .*

219 We can now state a variation of Whitney’s alignment result, see [27, Section IV.15].

220 ► **Lemma 12** (Whitney’s angle bound). *Suppose  $\sigma$  is a  $j$ -simplex of  $\mathbb{R}^d$ ,  $j < d$ , whose vertices*  
 221 *all lie within a distance  $d_{max}$  from a  $k$ -dimensional affine space  $A_0 \subset \mathbb{R}^d$  with  $k \geq j$ . Then*

$$222 \quad \sin \angle(\text{aff}(\sigma), A_0) \leq \frac{(j+1)d_{max}}{\min \text{alt}(\sigma)}.$$

223 **Simplices in a star in a triangulation of type  $\tilde{\mathbf{A}}_d$ .** The precise number of simplices  
 224 in the star of a vertex plays an important role in the volume estimates in Section 5. We will  
 225 now give an explicit bound on this number.

226 In general the  $(d - k)$ -faces of a Voronoi cell correspond to the  $k$ -faces in the Delaunay  
 227 dual. The triangulation  $\mathcal{T}$  is Delaunay and the dual of a vertex is a permutahedron, see  
 228 [13]. We now remind ourselves of the following definition, see [2], and lemma:

229 ► **Definition 13.** Let  $S(d, k)$  be the Stirling number of the second kind, which is the number  
 230 of ways to partition a set of  $d$  elements into  $k$  non-empty subsets, that is

$$231 \quad S(d, k) = \frac{1}{k!} \sum_{j=0}^k (-1)^j \binom{k}{j} (k - j)^d.$$

232 ► **Corollary 14** (Corollary 3.15 of [22]). *The number of  $(d + 1 - k)$ -faces of the permutahedron*  
 233 *is  $k!S(d + 1, k)$ .*

234 By duality, the lemma immediately gives us the number  $N_k$  of  $k$ -faces that contain a given  
 235 vertex in  $\mathcal{T}$ ,  $N_k = k!S(d + 1, k)$ . We also write

$$236 \quad N_{\leq k} = 2 + \sum_{j=1}^k j!S(d + 1, j), \tag{3}$$

237 which is an upper bound on the total number of faces of dimension less or equal to  $k$  that  
 238 contain a given vertex. We have added 2 because we want to have a safety margin if we  
 239 have to consider the empty set (as will be apparent in (16)), and have a strict inequality.  
 240 We now claim the following:

241 ► **Claim 15.** *We have  $N_{\leq k} \lesssim k^d d^k$ .*



242 **5 Perturbing the ambient triangulation**

243 This section is dedicated to the perturbation of the Coxeter triangulation such that the  
 244 manifold is sufficiently far from the simplices of dimension at most  $d - n - 1$  in  $\tilde{\mathcal{T}}$ .

- 245 ■ In Section 5.1, we prove that it is possible to perturb the points as described in the second  
 246 step of part 1 of the algorithm. This involves a significant amount of volume estimates,  
 247 which are now completely quantized. Indicate how fine the ambient triangulation  $\mathcal{T}$  has  
 248 to be compared to  $\text{rch}(\mathcal{M})$
- 249 ■ In Section 5.2, we define the perturbation and prove that this in fact gives a triangulation  
 250 for which the low dimensional simplices lie sufficiently far from the manifold.

251 The proofs of the results in Section 5.2 rely on Appendix A. We shall indicate the correspond-  
 252 ing sections in Whitney [27] between brackets in the title of the section, when appropriate.

253 **5.1 The complex  $\tilde{\mathcal{T}}$  (Section IV.18 of [27])**

254 Before we can dive into the algorithmic construction of the perturbed complex  $\tilde{\mathcal{T}}$ , we need  
 255 to fix some constants and give some explicit bounds on the constants.

256 **Balls and exclusion volumes.** Let  $B^d(r)$  be any ball in  $\mathbb{R}^d$  of radius  $r$ . We now define  
 257  $\bar{\rho}_1 > 0$  as follows: For any two parallel  $(d - 1)$ -hyperplanes whose distance apart is less  
 258 than  $2\bar{\rho}_1 r$ , the intersection of the slab between the two hyperplanes with the ball  $B^d(r)$  is  
 259 denoted by  $\mathcal{S}$ . Now,  $\bar{\rho}_1$  is the largest number such that the volume ( $\text{vol}$ ) of any  $\mathcal{S}$  satisfies

260 
$$\text{vol}(\mathcal{S}) \leq \frac{\text{vol}(B^d(r))}{2N_{\leq d-n-1}},$$

261 with  $N_{\leq d-n}$  as in (3). A precise bound on  $\bar{\rho}_1$  can be given, see Remark 35 in Appendix C.  
 262 We will use an easier bound  $\rho_1$ , at the cost of weakening the result:

263 ► **Lemma 16.** *We have*

264 
$$\bar{\rho}_1 \geq \rho_1 = \begin{cases} \frac{2^{2k-2}(k!)^2}{\pi(2k)!N_{\leq d-n-1}} & \text{if } d = 2k \\ \frac{(2k)!}{2^{2k+2}k!(k-1)!N_{\leq d-n-1}} & \text{if } d = 2k - 1. \end{cases} \quad (4)$$

265 *Note that*

266 
$$\rho_1 \sim \frac{1}{\sqrt{d}N_{\leq d-n-1}}.$$

267 **The coarseness of  $\mathcal{T}$ .** As mentioned, we perturb the vertices of a Coxeter triangulation.  
 268 The maximal distance between an unperturbed vertex  $v_i$  and the associated perturbed vertex  
 269  $\tilde{v}_i$  is  $\tilde{c}L$ . We will assume that  $\tilde{c}$  satisfies the bounds below in (14).

270 We are now ready to introduce the demands on the triangulation of ambient space. We  
 271 start by bounding the scale of the Coxeter triangulation  $\mathcal{T}$  by bounding the longest edge  
 272 length. We do this by giving some constants. We define  $\alpha_1$  and  $\alpha_k$  by a recursion relation  
 273 as follows

274 
$$\alpha_1 = \frac{4}{3}\rho_1\tilde{c} \qquad \frac{2}{3}\alpha_{k-1}\tilde{c}\rho_1 = \alpha_k, \quad (5)$$

275 that is  $\alpha_k = \frac{2^{k+1}}{3^k} \rho_1^k \tilde{c}^k$ . These definitions play an essential role in the volume estimates for  
 276 the perturbation of the vertices, that are necessary to guarantee quality. Note that  $\alpha_k$  is  
 277 extremely small. In particular, we shall have that

$$278 \quad \alpha_k \leq \frac{1}{18^k}, \tag{6}$$

279 because of the way that  $\tilde{c}$  will be chosen, see (15),  $\rho_1$  is also very small. Furthermore we  
 280 notice that  $\alpha_k < \alpha_{k-1}$ . To make sure the formulae do not become too big, we introduce the  
 281 notation

$$282 \quad \zeta = \frac{8}{15\sqrt{d} \binom{d}{d-n} \cdot (1 + 2\tilde{c})} \left(1 - \frac{8\tilde{c}}{t(\mathcal{T})^2}\right) t(\mathcal{T}). \tag{7}$$

283 Note that  $\zeta$  depends on both the ambient and intrinsic dimension and the perturbation  
 284 parameter  $\tilde{c}$ . We set the coarseness of the ambient triangulation by demanding that  $L$   
 285 satisfies

$$286 \quad \left(1 - \sqrt{1 - \left(\frac{6L(\mathcal{T})}{\text{rch}(\mathcal{M})}\right)^2}\right) \text{rch}(\mathcal{M}) = \frac{(\alpha_{d-n})^{4+2n}}{6(n+1)^2} \zeta^{2n} L, \tag{8}$$

287 or equivalently

$$288 \quad \frac{L}{\text{rch}(\mathcal{M})} = \frac{2 \frac{(\alpha_{d-n})^{4+2n}}{6(n+1)^2} \zeta^{2n}}{\left(\frac{(\alpha_{d-n})^{4+2n}}{6(n+1)^2} \zeta^{2n}\right)^2 + 6^2}. \tag{9}$$

289 Note that

$$290 \quad \frac{L}{\text{rch}(\mathcal{M})} < \frac{(\alpha_{d-n})^{4+2n}}{54(n+1)^2} \zeta^{2n} < \frac{(\alpha_{d-n})^2}{54}, \quad \frac{(\alpha_{d-n})^{4+2n}}{6(n+1)^2} \zeta^{2n} < \frac{(\alpha_{d-n})^2}{3} \leq \frac{\alpha_{d-n}}{3}, \tag{10}$$

291 which will be often used below to simplify expressions.

292 ► **Remark.** We have to choose the right hand side in (8) very small, because the bounds on  
 293 the quality of the simplices that will make up the triangulations are very weak. The details  
 294 of these estimates can be found in Lemma 26.

295 **( $d - n - 1$ )-skeleton safe triangulations.** We shall denote the simplices by  $\tau$  and  
 296  $\sigma$ . We will use lower indices to distinguish simplices, while upper indices will stress the  
 297 dimension, for example  $\tau_j^k$  is a simplex of dimension  $k$ .

298 ► **Definition 17** ( $(d - n - 1)$ -skeleton safe triangulations). We say that a perturbed trian-  
 299 gulation  $\tilde{\mathcal{T}}$  of  $\mathcal{T}$  in  $\mathbb{R}^d$  is  $(d - n - 1)$ -skeleton safe with respect to the  $n$ -dimensional manifold  
 300  $\mathcal{M}$  if

$$301 \quad d(\tau^k, \mathcal{M}) > \alpha_k L, \tag{11}$$

302 for all faces  $\tau^k$  in  $\tilde{\mathcal{T}}$ , with  $k \leq d - n - 1$ , and

$$303 \quad \tilde{L} < \frac{13}{12} L \tag{12}$$

$$304 \quad t(\tilde{\mathcal{T}}) \geq \frac{4}{5\sqrt{d}} \left(1 - \frac{8\tilde{c}}{t(\mathcal{T})^2}\right) t(\mathcal{T}). \tag{13}$$

305 **5.2 Perturbing the vertices (Section IV.18)**

306 We now discuss the details of the perturbation scheme that we described in the algorithm  
 307 section. The perturbation scheme follows Whitney and is inductive.

308 **Construction of  $\tilde{\mathcal{T}}$ .** Let  $v_1, v_2, \dots$  be the vertices of  $\mathcal{T}$ , we are going to inductively  
 309 choose new vertices  $\tilde{v}_1, \tilde{v}_2, \dots$  for  $\tilde{\mathcal{T}}$ , with

$$310 \quad |v_i - \tilde{v}_i| \leq \tilde{c}L = \min \left\{ \frac{t(\mathcal{T})\mu_0}{18d} \delta, \frac{1}{24} t(\mathcal{T})^2 L \right\}, \quad (14)$$

311 using the notation of Section 4. Notice that because  $t(\mathcal{T}) \leq 1$ , by definition of the thickness  
 312 of a simplex, we have

$$313 \quad \tilde{c} \leq \frac{1}{24}. \quad (15)$$

314 With this bound we immediately have that (12) is satisfied. We also claim the following:

315 **► Claim 18.**  *$\tilde{\mathcal{T}}$  has the same combinatorial structure as  $\mathcal{T}$ . Moreover, (13) is satisfied.*

316 We now give the scheme where the vertices are perturbed inductively. Suppose that the  
 317 vertices  $\tilde{v}_1, \dots, \tilde{v}_{i-1}$  have been determined, and thus the complex  $\tilde{\mathcal{T}}_{i-1}$  with these vertices.  
 318 A simplex  $\{\tilde{v}_{j_1} \dots \tilde{v}_{j_k}\}$  lies in  $\tilde{\mathcal{T}}_{i-1}$  if and only if  $\{v_{j_1} \dots v_{j_k}\}$  lies in  $\mathcal{T}$ . We shall now find  
 319  $\tilde{v}_i$  and thus  $\tilde{\mathcal{T}}_i$  so that for any  $\tau^k \in \tilde{\mathcal{T}}_i$  of dimension  $k \leq d - n - 1$ , (11) is satisfied. We  
 320 distinguish two cases:

321 **Case 1.** The distance  $d(v_i, \mathcal{M})$  is greater than  $\frac{3}{2}L$ . In this case we choose  $\tilde{v}_i = v_i$ . The  
 322 inequality (11) now follows, because  $\tilde{L} < (1 + 2\tilde{c})L$  and thus by the triangle inequality any  
 323 simplex in  $\tilde{\mathcal{T}}$  with vertex  $v_i$  is at least distance  $(\frac{1}{2} - 2\tilde{c})L > \frac{5}{12}L$  from the manifold, which  
 324 is much larger than  $\alpha_k L < \frac{1}{18^k} L$ .

325 **Case 2.** The distance  $d(v_i, \mathcal{M})$  is smaller than  $\frac{3}{2}L$ . Let  $p$  be a point in  $\mathcal{M}$  such that  
 326  $d(v_i, p) < \frac{3}{2}L$ . Let

$$327 \quad \tau'_0 (= \emptyset), \tau'_1, \dots, \tau'_\nu \quad (16)$$

328 be the simplices of  $\tilde{\mathcal{T}}_{i-1}$  such that the joins  $\tau_j = \tau'_j * \tilde{v}_i$  are simplices of  $\tilde{\mathcal{T}}$ , and  $\dim(\tau'_j * \tilde{v}_i) \leq$   
 329  $d - n - 1$  (and thus  $\dim(\tau'_j) \leq d - n - 2$ ), with  $0 \leq j \leq \nu$ . We note that  $\nu \leq N_{\leq d-n-1}$ ,  
 330 with  $N_{\leq k}$  as defined in (3). We now consider the span, denoted by  $\text{span}(\tau'_j, T_p \mathcal{M})$ , for all  
 331  $0 \leq j \leq \nu$ . Note that the dimension of  $\text{span}(\tau'_j, T_p \mathcal{M})$  is at most  $(d - n - 2) + n + 1 = d - 1$ .

332 We now claim the following:

333 **► Claim 19.** *We can pick  $\tilde{v}_i$  such that it lies sufficiently far from each  $\text{span}(\tau'_j, T_p \mathcal{M})$ , that  
 334 is*

$$335 \quad d(\tilde{v}_i, \text{span}(\tau'_j, T_p \mathcal{M})) \geq \rho_1 \tilde{c}L, \quad (17)$$

336 *while it is not too far from  $v_i$ , that is  $|\tilde{v}_i - v_i| \leq \tilde{c}L$ .*

337 The following claim completes Case 2 and establishes that the triangulation is  $(d - n - 1)$ -  
 338 skeleton safe:

339 **► Claim 20.** *(11) is satisfied.*

340 We emphasize that in the perturbation of the points it suffices to look at the tangent  
 341 spaces at specific points, making this constructive proof an algorithm.

342 **6** Constructing the triangulation of  $\mathcal{M}$

343 Section 6.1 gives geometric consequences of the perturbation we discussed in the previous  
 344 section. Most importantly we shall see that the intersections of simplices in  $\tilde{\mathcal{T}}$  with  $\mathcal{M}$  and  
 345 those of simplices in  $\tilde{\mathcal{T}}$  with the tangent space of  $\mathcal{M}$  at a nearby point are equivalent. Here  
 346 we again rely on Appendix A. The triangulation  $K$  of  $\mathcal{M}$  is defined in Section 6.2.

347 **6.1** The geometry of the intersection of simplices in  $\tilde{\mathcal{T}}$  and  $\mathcal{M}$

348 In this section, we discuss the geometry of simplices in  $\tilde{\mathcal{T}}$  in relation to  $\mathcal{M}$ . We follow [27,  
 349 Section IV.19], with the usual exceptions of the use of Coxeter triangulations, the thickness,  
 350 and the reach to quantify the results. The proofs below also differ in a fair number of places  
 351 from the original.

352 We first establish a lower bound on the distance between  $T_p\mathcal{M}$  and simplices in the  
 353  $(d - n - 1)$ -skeleton of  $\mathcal{T}^P$  that are close to  $p$ .

354 **► Lemma 21.** *Let  $p \in \mathcal{M}$  and suppose that  $\tau^k \in \tilde{\mathcal{T}}$ , with  $k \leq d - n - 1$ , such that*  
 355  *$\tau^k \subset B(p, 6L)$ , then*

356 
$$d(\tau^k, T_p\mathcal{M}) > \frac{2}{3}\alpha_k L.$$

357 We can now examine the relation between intersections with the manifold and nearby  
 358 tangent spaces.

359 **► Lemma 22.** *Suppose that  $\mathcal{M}$  intersects  $\tau^k \in \tilde{\mathcal{T}}$ . Let  $p \in \mathcal{M}$ , such that  $\tau^k \subset B(p, 6(L))$ ,*  
 360 *then  $T_p\mathcal{M}$  intersects  $\tau^k$ .*

361 We can now bound the angle between simplices and tangent spaces.

362 **► Lemma 23.** *Suppose that  $\mathcal{M}$  intersects  $\tau^k \in \tilde{\mathcal{T}}$  and  $\tau^k$  has dimension  $d - n$ , that is*  
 363  *$k = d - n$ . Let  $p \in \mathcal{M}$ , such that  $\tau^k \subset B(p, 6L)$ , then*

364 
$$\sin \angle(\text{aff}(\tau^k), T_p\mathcal{M}) \geq \frac{2d(T_p\mathcal{M}, \partial\tau^k)}{L + 2\tilde{c}L} \geq \frac{\frac{4}{3}\alpha_k L}{L + 2\tilde{c}L} \geq \frac{16}{10}\alpha_k.$$

365 Below we investigate the relation between intersections of tangent spaces and simplices  
 366 and intersections between the manifold and simplices. We combine two statements of Section  
 367 IV.19 in the following lemma. The proof is quite different from the original.

368 **► Lemma 24.** *If  $p \in \mathcal{M}$ ,  $\tau^k \in \tilde{\mathcal{T}}$  and  $\tau^k \subset B(p, 6L)$ , and moreover  $T_p\mathcal{M}$  intersects  $\tau^k$ , then*  
 369  *$k \geq d - n$  and  $\mathcal{M}$  intersects  $\tau^k$ . If  $k = d - n$  this point is unique, which in particular means*  
 370 *that every simplex of dimension  $d - n$  contains at most one point of  $\mathcal{M}$*

371 Finally, we study the faces of a simplex that intersects  $\mathcal{M}$ . This is essential for the  
 372 barycentric subdivision in part 2 of the algorithm. The proof is identical to the original.

373 **► Lemma 25.** *If  $\mathcal{M}$  intersects  $\tau = \{v_0, \dots, v_r\} \in \tilde{\mathcal{T}}$ , then for each  $v_i \in \tau$ , there exists some*  
 374  *$(d - n)$ -face  $\tau'$  of  $\tau$  such that  $v_i \in \tau'$  and  $\tau'$  intersects  $\mathcal{M}$ .*

375 **6.2 The triangulation of  $\mathcal{M}$ : The complex  $K$  (Section IV.20 of [27])**

376 The construction of the complex follows Section IV.20 of [27].

377 In each simplex  $\tau$  of  $\tilde{\mathcal{T}}$  that intersects  $\mathcal{M}$  we choose a point  $v(\tau)$  and construct a complex  
378  $K$  with these points as vertices. The construction goes via barycentric subdivision. For each  
379 sequence  $\tau_0 \subset \tau_1 \subset \dots \subset \tau_k$  of distinct simplices in  $\tilde{\mathcal{T}}$  such that  $\tau_0$  intersects  $\mathcal{M}$ ,

380 
$$\sigma^k = \{v(\tau_0), \dots, v(\tau_k)\} \tag{18}$$

381 will be a simplex of  $K$ . The definition of  $v(\tau)$  depends on the dimension of  $\tau$ :382 ■ If  $\tau$  is a simplex of dimension  $d - n$ , then there is a unique point of intersection with  
383  $\mathcal{M}$ , due to Lemma 24. We define  $v(\tau)$  to be this unique point.384 ■ If  $\tau$  has dimension greater than  $d - n$ , then we consider the faces  $\tau_1^{d-n}, \dots, \tau_j^{d-n}$  of  $\tau$   
385 of dimension  $d - n$  that intersect  $\mathcal{M}$ . These faces exist thanks to Lemma 25. We now  
386 define  $v(\tau)$  as follows:

387 
$$v(\tau) = \frac{1}{j} (v(\tau_1^{d-n}) + \dots + v(\tau_j^{d-n})). \tag{19}$$

388 ► **Remark.** We stress that thanks to Lemma 24, choosing the point  $v(\tau^{d-n})$  to be the point of  
389 intersection with  $T_p\mathcal{M}$ , assuming  $p$  is sufficiently close, locally gives the same combinatorial  
390 structure as intersections with  $\mathcal{M}$ . We also stress that for the combinatorial structure it  
391 does not really matter where  $\mathcal{M}$  intersects a simplex of  $\tilde{\mathcal{T}}$ , as long as it does.392 We can now prove the following bound on the altitudes of the simplices we constructed  
393 in this manner.394 ► **Lemma 26.** *Let  $\sigma^n$  be a top dimensional simplex as defined in (18), then*

395 
$$\min \text{alt}(\sigma^n) > \zeta^n (\alpha_{d-n-1})^n \tilde{L},$$

396 *where  $\min \text{alt}$  denotes the minimal altitude or height, and we used the notation  $\zeta$ , as defined*  
397 *in (7).*398 **7 The triangulation proof**399 Given the triangulation  $\tilde{\mathcal{T}}$ , we want to prove that the intersection of  $\mathcal{M} \cap \tau^d$  is homeomorphic  
400 to the triangulated polytope described in Section 6.2. This immediately gives a global  
401 homeomorphism between the triangulation and the manifold.402 The homeomorphism we discuss in this section differs greatly from Whitney's own ap-  
403 proach. Firstly, he used the closest point projection as a map (which does not respect  
404 simplices, meaning that the point in  $K$  and its projection may lie in different simplices of  
405  $\tilde{\mathcal{T}}$ ). Secondly, to prove that this map is a homeomorphism, he uses what has become known  
406 as Whitney's lemma in much the same way as in [8].407 The great advantage of our approach to the homeomorphism proof is that it is extremely  
408 explicit and it is elementary in the sense that it does not rely on topological results. We also  
409 need precise bounds on the angles, which do not require deep theory, but are quite intricate.410 Because we work with an ambient triangulation of type  $\tilde{A}$  and we do not perturb too  
411 much, the simplices of  $\tilde{\mathcal{T}}$  are Delaunay. The homeomorphism from  $\mathcal{M} \cap \tau^d$  to the triangulated  
412 polytope  $K \cap \tau^d$ , with  $K$  as defined in Section 6.2 and  $\tau^d \in \tilde{\mathcal{T}}$ , gives that the intersection  
413 of any simplex in  $\tilde{\mathcal{T}}$  with  $\mathcal{M}$  is a topological ball of the appropriate dimension. This may  
414 remind the reader of the closed ball property of Edelsbrunner and Shah [18].

415 **Overview homeomorphism proof.** The homeomorphism proof consists of three steps:

- 416 ■ For each maximal simplex  $\tau \in \tilde{\mathcal{T}}$  we provide a ‘tubular neighbourhood’ for  $K \cap \tau$  adapted
- 417 to  $\tau$ . By this we mean that, for each point  $\bar{p}$  in  $K \cap \tau$ , we designate a ‘normal’ space  $\mathcal{N}_{\bar{p}}$
- 418 that has dimension equal to the codimension of  $\mathcal{M}$  and  $K$  and is transversal to  $K \cap \tau$ .
- 419 Moreover, these directions shall be chosen in a sufficiently controlled and smooth way,
- 420 so that every point  $x$  in  $\tau$  that is sufficiently close to  $K$  has a unique point  $\bar{p}$  on  $K \cap \tau$
- 421 such that  $x - \bar{p} \in \mathcal{N}_{\bar{p}}$ .
- 422 ■ We give conditions that enforce that the ‘normal’ spaces  $\mathcal{N}_{\bar{p}}$  intersect  $\mathcal{M}$  transversely.
- 423 More precisely, we prove that the angle between  $\tilde{N}_{\bar{p}}$  and  $N_q\mathcal{M}$ , for any  $q \in \mathcal{M} \cap \tau$  is
- 424 upper bounded by a quantity strictly less than 90 degrees.
- 425 ■ We conclude that the projection along  $\mathcal{N}_{\bar{p}}$  gives a homeomorphism from  $\mathcal{M}$  to  $K$ .

### 426 7.1 Constructing the tubular neighbourhood

427 We now give the construction of the ‘tubular neighbourhood’ of  $K$ . We use two results from

428 the previous sections:

- 429 ■ The normal space is almost constant, see Lemma 2, near a simplex  $\tau \in \tilde{\mathcal{T}}$ , because it is
- 430 small. So  $T\mathcal{M}$  and  $N\mathcal{M}$  near  $p$  are well approximated by  $T_p\mathcal{M}$  and  $N_p\mathcal{M}$ .
- 431 ■ The angles between the normal space and those faces  $\tau_k^{d-n}$  of dimension  $d - n$  that
- 432 intersect  $\mathcal{M}$  are bounded from below by Lemma 23.

433 This means that the orthogonal projection map  $\pi_{\text{aff}(\tau_k^{d-n}) \rightarrow N_p\mathcal{M}} = \pi_{\tau_k^{d-n}}$  from the affine hull

434  $\text{aff}(\tau_k^{d-n})$  to  $N_p\mathcal{M}$  is a (linear) bijection. Now note that the orthonormal basis  $e_1, \dots, e_{d-n}$

435 of  $N_p\mathcal{M}$  induces a (generally not orthonormal) basis of  $\text{aff}(\tau_k^{d-n})$  under the inverse image

436 of the map  $\pi_{\tau_k^{d-n}}$ , denoted by  $\{\pi_{\tau_k^{d-n}}^{-1}(e_j) \mid j = 1, \dots, d - n\}$ .

437 We can now define the normal spaces for the complex  $K$ . We first do this for the vertices

438  $v(\tau^{d-n})$  (these vertices lie on  $\mathcal{M}$ ), secondly for general vertices of  $K$  (these vertices do not

439 necessarily lie on  $\mathcal{M}$ ) and finally using barycentric coordinates for arbitrary points in  $K$ .

440 Having defined a basis of  $\text{aff}(\tau_k^{d-n})$  for the vertices  $v(\tau_k^{d-n})$ , as defined in Section 6.2,

441 we can construct a basis of a  $(d - n)$ -dimensional affine space, through each  $v(\tau)$ . The

442 construction is similar to that of Section 6.2. If  $\tau$  has dimension greater than  $d - n$ , then

443 we consider the faces  $\tau_1^{d-n}, \dots, \tau_j^{d-n}$  of  $\tau$  of dimension  $d - n$  that intersect  $\mathcal{M}$ . For each

444  $e_i \in N_p\mathcal{M}$ , we write

$$445 \quad N_{v(\tau)}(e_i) = \frac{1}{j} \left( \pi_{\tau_1^{d-n}}^{-1}(e_i) + \dots + \pi_{\tau_j^{d-n}}^{-1}(e_i) \right). \tag{20}$$

446 Using these vectors we can define the space  $\mathcal{N}_{v(\tau)} = \text{span}(N_{v(\tau)}(e_i))$ .

447 Let  $\sigma^n = \{v(\tau_0^{d-n}), \dots, v(\tau_n^d)\}$  be a simplex of  $K$ . For any point  $\bar{p}$  in  $\sigma^n$ , with barycentric

448 coordinates  $\lambda = (\lambda_0, \dots, \lambda_n)$ , we define

$$449 \quad N_{\bar{p}}(e_i) = \lambda_0 N_{v(\tau_0^{d-n})}(e_i) + \dots + \lambda_n N_{v(\tau_n^{d-n})}(e_i). \tag{21}$$

450 By defining  $\mathcal{N}_{\bar{p}} = \text{span}(N_{\bar{p}}(e_i))$ , we get affine spaces for each point in each  $\sigma^n \in K$ .

451 ► **Remark.** By construction, these spaces are consistent on the faces of simplices in  $K$  as

452 well as with the boundaries of the  $d$  dimensional simplices in  $\tilde{\mathcal{T}}$ .

453 **7.2 The size of the tubular neighbourhoods and the homeomorphism**454 In this section, we establish the size of the neighbourhood of  $K$  as defined by  $\mathcal{N}_{\bar{p}}$ .455 The following angle estimate is an essential part of the estimate of the size of the neigh-  
456 bourhood of the triangulation  $K$ .457 **► Lemma 27.** *Suppose that  $p \in \mathcal{M}$ ,  $\tau^d \subset B(p, 6L)$  and  $\sigma^n \in K$  such that  $\sigma^n \subset \tau^d$ , where  
458 we regard  $\sigma^n$  and  $\tau^d$  as subsets of  $\mathbb{R}^d$ . Then the angle between  $T_p\mathcal{M}$  and  $\text{aff}(\sigma^n)$  is bounded  
459 as follows:*

460 
$$\sin \angle(\text{aff}(\sigma^n), T_p\mathcal{M}) \leq \frac{(\alpha_{d-n})^{4+n}}{6(n+1)} \zeta^n.$$

461 With this we can give a bound on the size of the neighbourhood of  $K$ .462 **► Lemma 28.** *Let  $\bar{p}, \bar{q} \in \sigma^n$ , with barycentric coordinates  $\lambda = (\lambda_0, \dots, \lambda_n)$ ,  $\lambda' = (\lambda'_0, \dots, \lambda'_n)$   
463 respectively. Suppose that  $\mathcal{N}_{\bar{p}}$  and  $\mathcal{N}_{\bar{q}}$  be as defined in Section 7.1. Suppose now that the  
464 intersection between  $\bar{p} + \mathcal{N}_{\bar{p}}$  and  $\bar{q} + \mathcal{N}_{\bar{q}}$  is non-empty. Here  $\bar{p} + \mathcal{N}_{\bar{p}}$  and  $\bar{q} + \mathcal{N}_{\bar{q}}$  denote the affine  
465 spaces that go through  $\bar{p}$ ,  $\bar{q}$  and are parallel to  $\mathcal{N}_{\bar{p}}$ ,  $\mathcal{N}_{\bar{q}}$ , respectively. If  $x \in \bar{p} + \mathcal{N}_{\bar{p}} \cap \bar{q} + \mathcal{N}_{\bar{q}}$ ,  
466 then*

467 
$$d(x, \text{aff}(\sigma^n)) \geq \frac{\left(\frac{16}{10}\right)^2 (\alpha_{d-n})^4}{n+1} \zeta^n (\alpha_{d-n-1})^n \tilde{L}.$$

468 *Because, by construction, the  $\mathcal{N}_{\bar{p}}$  agree on the faces of the  $n$ -dimensional simplices in  $K$ ,  
469 this provides a tubular neighbourhood for  $K$  of this size.*470 **► Lemma 29.** *Suppose  $\tau^d \in \tilde{\mathcal{T}}$  and that  $\mathcal{M} \cap \tau^d \neq \emptyset$ . Then,  $\mathcal{M} \cap \tau^d$  lies in the tubular  
471 neighbourhood of  $K \cap \tau^d$  as defined in Section 7.1.*472 Having established that  $\mathcal{M}$  lies in the tubular neighbourhood around  $K$  we can sensibly  
473 speak about the projection from  $\mathcal{M}$  to  $K$  along the direction  $N$ . Because we also have that  
474 the projection from  $\mathcal{M}$  to  $K$  in the direction  $\mathcal{N}$  (as defined in Section 7.1) is transversal  
475 (Because  $\pi/2$  minus the angle between  $\mathcal{N}_{\bar{p}}$  and  $N_p\mathcal{M}$ , see (33), is much bigger than the  
476 variation of the tangent/normal space as bounded by Lemma 2 and (9)) we see that  $\mathcal{M} \cap \tau^d$   
477 is homeomorphic to  $K \cap \tau^d$ . By construction the projection map is compatible on the  
478 boundaries of  $\tau^d$ , so we also immediately have an explicit homeomorphism between  $\mathcal{M}$  and  
479  $K$ . This completes the proof of Theorem 1. We emphasize that along the way we have also  
480 given a bounds on

- 481
- the Hausdorff distance between  $\mathcal{M}$  and  $K$  (Lemmas 29 and 28)
  - 482 ■ the quality (Lemma 26)
  - 483 ■ the variation of the tangent spaces ((33), Lemma 2 and (9) as mentioned above).

484 **References**

- 485
- 1 E. Aamari and C. Levrard. Non-Asymptotic Rates for Manifold, Tangent Space, and  
486 Curvature Estimation. *ArXiv e-prints*, May 2017. arXiv:1705.00989.
  - 487 2 Milton Abramowitz and Irene A. Stegun. *Handbook of mathematical functions : with*  
488 *formulas, graphs, and mathematical tables*. National Bureau of Standards, 1970.
  - 489 3 N. Amenta and M. W. Bern. Surface reconstruction by Voronoi filtering. In *SoCG*, pages  
490 39–48, 1998. URL: [citeseer.ist.psu.edu/amenta98surface.html](http://citeseer.ist.psu.edu/amenta98surface.html).

- 491 **4** N. Amenta, M. W. Bern, and M. Kamvysselis. A new Voronoi-based surface reconstruction  
492 algorithm. In *ACM SIGGRAPH*, pages 415–421, 1998.
- 493 **5** J.-D. Boissonnat, R. Dyer, and A. Ghosh. The stability of Delaunay triangulations. *Inter-  
494 national Journal of Computational Geometry & Applications*, 23(04n05):303–333, 2013.
- 495 **6** J.-D. Boissonnat, R. Dyer, and A. Ghosh. Delaunay stability via perturbations. *Intern-  
496 ational Journal of Computational Geometry & Applications*, 24(02):125–152, 2014.
- 497 **7** Jean-Daniel Boissonnat, Frédéric Chazal, and Mariette Yvinec. *Geometric and Topological  
498 Inference*. Cambridge Texts in Applied Mathematics. Cambridge University Press, 2018.  
499 doi:10.1017/9781108297806.
- 500 **8** Jean-Daniel Boissonnat, Ramsay Dyer, Arijit Ghosh, and Mathijs Wintraecken. Local  
501 Criteria for Triangulation of Manifolds. In Bettina Speckmann and Csaba D. Tóth, edit-  
502 ors, *34th International Symposium on Computational Geometry (SoCG 2018)*, volume 99  
503 of *Leibniz International Proceedings in Informatics (LIPIcs)*, pages 9:1–9:14, Dagstuhl,  
504 Germany, 2018. Schloss Dagstuhl–Leibniz-Zentrum fuer Informatik. URL: [http://drops.  
505 dagstuhl.de/opus/volltexte/2018/8722](http://drops.dagstuhl.de/opus/volltexte/2018/8722), doi:10.4230/LIPIcs.SoCG.2018.9.
- 506 **9** Jean-Daniel Boissonnat and Arijit Ghosh. Manifold reconstruction using tangential  
507 Delaunay complexes. *Discrete & Computational Geometry*, pages 221–267, 2014.
- 508 **10** Jean-Daniel Boissonnat, André Lieutier, and Mathijs Wintraecken. The Reach, Met-  
509 ric Distortion, Geodesic Convexity and the Variation of Tangent Spaces. In Bettina  
510 Speckmann and Csaba D. Tóth, editors, *34th International Symposium on Computational  
511 Geometry (SoCG 2018)*, volume 99 of *Leibniz International Proceedings in Informatics  
512 (LIPIcs)*, pages 10:1–10:14, Dagstuhl, Germany, 2018. Schloss Dagstuhl–Leibniz-Zentrum  
513 fuer Informatik. URL: <http://drops.dagstuhl.de/opus/volltexte/2018/8723>, doi:  
514 10.4230/LIPIcs.SoCG.2018.10.
- 515 **11** S. S. Cairns. On the triangulation of regular loci. *Annals of Mathematics. Second Series*,  
516 35(3):579–587, 1934. doi:10.2307/1968752.
- 517 **12** S-W. Cheng, T. K. Dey, and E. A. Ramos. Manifold Reconstruction from Point Samples.  
518 In *Proc. ACM-SIAM Symp. Discrete Algorithms*, pages 1018–1027, 2005.
- 519 **13** Aruni Choudhary, Siargey Kachanovich, and Mathijs Wintraecken. Coxeter triangula-  
520 tions have good quality. HAL preprint, December 2017. URL: [https://hal.inria.fr/  
521 hal-01667404](https://hal.inria.fr/hal-01667404).
- 522 **14** H.S.M. Coxeter. Discrete groups generated by reflections. *Annals of Mathematics*, pages  
523 588–621, 1934.
- 524 **15** T. K. Dey. *Curve and Surface Reconstruction; Algorithms with Mathematical Analysis*.  
525 Cambridge University Press, 2007.
- 526 **16** J.J. Duistermaat and J.A.C. Kolk. *Multivariable Real Analysis II: Integration*. Cambridge  
527 University Press, 2004.
- 528 **17** R. Dyer, G. Vegter, and M. Wintraecken. Riemannian simplices and triangulations.  
529 *Geometriae Dedicata*, 179(1):91–138, 2015. (Preprint: arXiv:1406.3740). doi:10.1007/  
530 s10711-015-0069-5.
- 531 **18** H. Edelsbrunner and N. R. Shah. Triangulating topological spaces. In *SoCG*, pages 285–  
532 292, 1994.
- 533 **19** H. Federer. Curvature measures. *Trans. Amer. Math. Soc.*, 93(3):418–491, 1959.
- 534 **20** M. W. Hirsch. *Differential Topology*. Springer-Verlag, 1976.
- 535 **21** Albert T. Lundell and Stephen Weingram. *The Topology of CW Complexes*. Van Nostrand  
536 Reinhold Company, 1969.
- 537 **22** Maurice Maes and Bert Kappen. On the permutahedron and the quadratic placement  
538 problem. *Philips Journal of Research*, 46(6):267–292, 1992.
- 539 **23** P. Niyogi, S. Smale, and S. Weinberger. Finding the homology of submanifolds with high  
540 confidence from random samples. *Discrete & Comp. Geom.*, 39(1-3):419–441, 2008.



- 541 **24** B.C. Rennie and A.J. Dobson. On Stirling numbers of the second kind. *Journal of Combinatorial Theory*, 7(2):116 – 121, 1969. URL: <http://www.sciencedirect.com/science/article/pii/S0021980069800451>, doi:[https://doi.org/10.1016/S0021-9800\(69\)80045-1](https://doi.org/10.1016/S0021-9800(69)80045-1).
- 542  
543  
544
- 545 **25** J. G. Wendel. Note on the gamma function. *The American Mathematical Monthly*, 55(9):563–564, 1948. URL: <http://www.jstor.org/stable/2304460>.
- 546
- 547 **26** J. H. C. Whitehead. On  $C^1$ -complexes. *Annals of Mathematics*, 41(4):809–824, 1940. URL: <http://www.jstor.org/stable/1968861>.
- 548
- 549 **27** H. Whitney. *Geometric Integration Theory*. Princeton University Press, 1957.

## 550 **A** Some properties of affine spaces

551 In this appendix, we discuss two variants of lemmas from Appendix Section II.14 of [27],  
552 that are essential in the building of the triangulation, see Section 6.1 in particular. Both  
553 lemmas are due to Whitney. However, in both cases, the statement is different, because we  
554 prefer to work directly with angles and use the thickness as our quality measure. In the first  
555 case, the proof we provide differs significantly from the original. The first lemma will allow  
556 us to prove that if  $T_p\mathcal{M}$  intersects a simplex  $\tau \in \mathcal{T}$  and  $p$  and  $\tau$  are not too far from each  
557 other then  $\mathcal{M}$  intersects  $\tau$  and vice versa. The second result is essential in proving that  
558 the perturbation of the vertices as described in Section 2.1 part 1, gives a triangulation for  
559 which the low dimensional simplices are sufficiently far away from the manifold.

560 We start with a variation on Lemma 14a of Appendix Section II.14 of [27].

561 **► Lemma 30.** *Let  $\sigma$  be an  $s$ -simplex and  $A_0$  an affine  $n$ -dimensional subspace in  $\mathbb{R}^d$ . Assume*  
562 *that  $s + n \geq d$  and*

$$563 \quad d(A_0, \sigma) < d(A_0, \partial\sigma).$$

564 *Then  $s + n = d$ ,  $A$  intersects  $\sigma$  in a single point and*

$$565 \quad \sin \angle \text{aff}(\sigma)A_0 \geq 2d(A_0, \partial\sigma)/L(\sigma).$$

566 **Proof of Lemma 30.** Choose  $p \in \sigma$  and  $q \in A_0$  such that

$$567 \quad |p - q| = d(A_0, \sigma).$$

568 Now suppose that there is a vector  $v \neq 0$  that lies in the intersection of  $\text{aff}(\sigma)$  and  $A_0$ . Then  
569 there exists some  $c \in \mathbb{R}$  such that  $p + cv \in \partial\sigma$ . Because  $v$  lies in the intersection of  $\text{aff}(\sigma)$   
570 and  $A_0$ , we have that  $q + cv \in A_0$ . Clearly translation leaves distances invariant, so

$$571 \quad d(A_0, \sigma) = |p - q| = |(p + cv) - (q + cv)| \geq d(A_0, \partial\sigma),$$

572 which clearly contradicts the assumption. This means we can conclude that there is no such  
573  $v$  and therefore  $s + n = d$ .

574 Because there is no  $v$  in the intersection of  $\text{aff}(\sigma)$  and  $A_0$ , there is a unique point  $\bar{p}$  in this  
575 intersection. We'll now show that  $\bar{p} \in \sigma$ . I'll assume that  $\bar{p} \notin \sigma$ . This means in particular  
576 that  $q \neq \bar{p}$ . Because  $d(A_0, \sigma) < d(A_0, \partial\sigma)$ ,  $p - q$  is normal to  $\text{aff}(\sigma)$  and  $p \in \sigma \setminus \partial\sigma$ . Now  
577 consider the line from  $q$  to  $\bar{p}$ , which lies in  $A_0$ . The distance from a point on this line to  $\sigma$   
578 decreases (at least at first) as you go from  $q$  toward  $\bar{p}$ . This contradicts the definition of  $q$ .  
579 We conclude that  $\bar{p} \in \sigma$ .

580 Now suppose that  $l_0$  is a line in  $A_0$  that goes through  $\bar{p}$ . In order to derive a contradiction,  
 581 we assume that

582 
$$\sin \phi < 2d(A_0, \partial\sigma)/L(\sigma),$$

583 where  $\sin \phi$  denotes the angle between  $l_0$  and  $\text{aff}(\sigma)$ . Denote by  $\pi_{\text{aff}(\sigma)}(l_0)$  the orthogon-  
 584 al/closest point projection on  $\text{aff}(\sigma)$  of  $l_0$ . Because  $\bar{p} \in \sigma$   $\pi_{\text{aff}(\sigma)}(l_0)$  intersects  $\partial\sigma$  at a point  
 585  $\bar{q}$  and we may assume that  $|\bar{p} - \bar{q}| \leq \frac{1}{2}L(\sigma)$  so that  $l_0$  contains a point a distance

586 
$$\frac{1}{2}L(\sigma) \sin \phi < \frac{1}{2}L(\sigma)2d(A_0, \partial\sigma)/L(\sigma) = d(A_0, \partial\sigma)$$

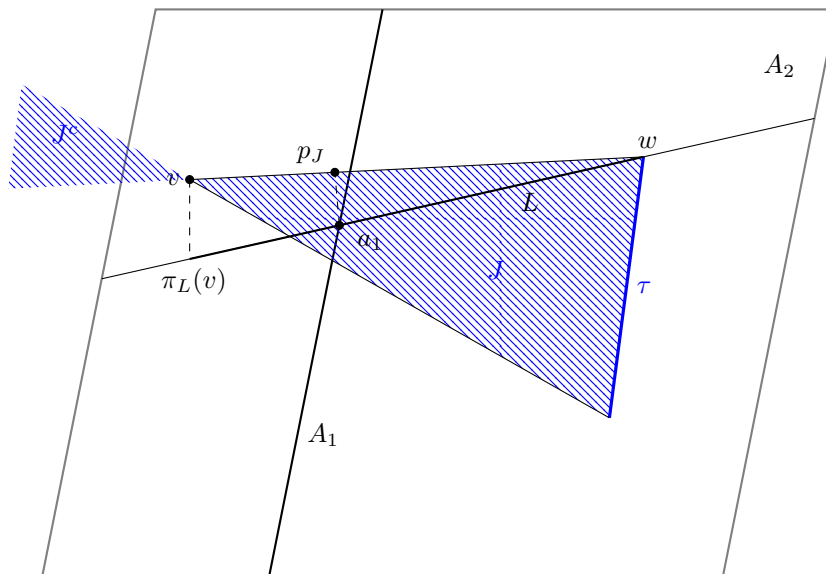
587 from  $\partial\sigma$ , a contradiction. Because  $l_0$  was an arbitrary line in  $A_0$  the result now follows. ◀

588 The following is a variation on Lemma 14b of Appendix Section II.14 of [27]. The proof  
 589 presented here is almost identical to the original.

590 ► **Lemma 31.** Let  $A_1$  and  $A_2$  be two affine subspaces in  $\mathbb{R}^d$ , with  $A_1 \subset A_2$ . Let  $\tau$  be a  
 591 simplex in  $A_2$ , and let  $v$  be a point in  $\mathbb{R}^d \setminus \tau$ . Define  $J$  to be the join of  $\tau$  and  $v$ . Then

592 
$$d(J, A_1) \geq \frac{d(\tau, A_1)d(v, A_2)}{L(J)}, \tag{22}$$

593 where the distances between sets are defined as  $d(B, C) = \inf_{x \in B, y \in C} |x - y|$  and  $L(J)$  denotes  
 594 the longest edge length of an edge in  $J$ .



595 ■ **Figure 2** Notation for the proof of Lemma 31.

596 **Proof of Lemma 31.** Let us suppose that (22) is false. Let  $J^c$  be the truncated cone that  
 597 consists of all half-lines that start at a point of  $\tau$  and pass through  $v$ . Then we may choose  
 598  $p_J \in J^c$  and  $a_1 \in A_1$  so that

599 
$$|p_J - a_1| = d(J^c, A_1),$$

600 by the definition of  $J^c$  and the hypothesis we also have

$$601 \quad d(J^c, A_1) \leq d(J, A_1) < \frac{d(\tau, A_1)d(v, A_2)}{L(J)}. \quad (23)$$

602 Now suppose that  $p_J$  lies on the half line that starts at  $w \in \tau$  and goes through  $v$ . Because  
 603  $\tau \subset A_2$ , we see that  $d(v, A_2) \leq L_e(J)$ . This means that (23) gives that  $d(J^c, A_1) < d(\tau, A_1)$ ,  
 604 so that  $p_J \neq w$ . We now immediately see that the line segment  $a_1p_J$  is orthogonal to the  
 605 line that goes through  $w$  and  $v$ , which extends the half line we mentioned above. Let  $\ell$  now  
 606 be the line that goes through  $a_1$  and  $w$ , and  $\pi_\ell(v) \in \ell$  the point that is closest to  $v$ . It  
 607 follows that  $\pi_\ell(v)w$  is perpendicular to  $\ell$ . Because  $a_1$  is nearer to  $p_J$  than  $w$ ,  $a_1$  and  $\pi_\ell(v)$   
 608 are on the same side of  $w$  in  $\ell$ . This means because two of the angles are the same (and  
 609 thus the third), that the triangles  $p_Jwa_1$  and  $\pi_\ell(v)wv$  are similar. We now have that

$$610 \quad d(J^c, A_1) = |p_J - a_1| = \frac{|a_1 - w||v - \pi_\ell(v)|}{|v - w|} \geq \frac{d(\tau, A_1)d(v, A_2)}{L(J)},$$

611 contradicting the hypothesis and thus proving the lemma.  $\blacktriangleleft$

## 612 **B** Remark on the $C^{1,1}$ case

613 We now first discuss a simpler version of 3. The result in this case is weaker, but can be  
 614 easily extended to the  $C^{1,1}$  setting as we shall see below.

615 The following consequence of Lemma 2 of is a stronger version of Lemma 5.4 of [23]:

616 **► Corollary 32.** *Suppose  $\mathcal{M}$  is  $C^2$  and  $p \in \mathcal{M}$ , then for all  $0 < r < \frac{\text{rch}(\mathcal{M})}{\sqrt{2}}$ , the projection  
 617  $\pi_{T_p\mathcal{M}}$  onto the tangent space  $T_p\mathcal{M}$ , restricted to  $\mathcal{M} \cap B(p, r)$  is a diffeomorphism onto its  
 618 image.*

619 **Proof of Corollary 32.** Let  $q \in \mathcal{M}$  such that  $|p - q| \leq r$ , then the differential of the projection  
 620 map  $\pi_{T_p\mathcal{M}}$  at  $q$  is non-degenerate, because, by Lemma 2, the angle  $\angle(T_p\mathcal{M}, T_q\mathcal{M})$  is less  
 621 than  $\pi/2$ . Because  $\mathcal{M} \cap B(p, r)$  is a topological ball of the right dimension by Proposition  
 622 1 of [10], the result now follows.  $\blacktriangleleft$

623 Similarly to Lemma 2 we have for  $C^{1,1}$  manifolds that:

624 **► Lemma 33** (Theorem 3 of [10]). *Now suppose that  $\mathcal{M}$  has positive reach, that is  $\mathcal{M}$  is at  
 625 least  $C^{1,1}$ , and let  $|p - q| \leq \text{rch}(\mathcal{M})/3$ , then*

$$626 \quad \sin \frac{\angle(T_p\mathcal{M}, T_q\mathcal{M})}{2} \leq \frac{1 - \sqrt{1 - \alpha^2}}{\sqrt{\frac{\alpha^2}{4} - (\frac{\alpha^2}{2} + 1 - \sqrt{1 - \alpha^2})^2}},$$

627 where  $\alpha = |p - q|/\text{rch}(\mathcal{M})$ .

628 This lemma gives us a corollary, which is the equivalent of Corollary 32:

629 **► Corollary 34.** *Suppose  $\mathcal{M}$  is  $C^{1,1}$  and  $p \in \mathcal{M}$ , then for all  $r < \frac{\text{rch}(\mathcal{M})}{3}$ , the projection  
 630  $\pi_{T_p\mathcal{M}}$  onto the tangent space  $T_p\mathcal{M}$ , restricted to  $\mathcal{M} \cap B(p, r)$  is a diffeomorphism onto its  
 631 image.*

632 These are in fact all the fundamental results that are needed to be able to extend to the  
 633  $C^{1,1}$  setting.

634 Assuming the manifold is  $C^{1,1}$  would lead to minor changes in the calculations in the  
 635 proof of Lemma 24 and would in theory influence the final conclusion in Section 7.2. However,  
 636 because we have a significant margin in the difference between  $\pi/2$  minus the angle between  
 637  $\mathcal{N}_{\bar{p}}$  and  $N_p\mathcal{M}$  we would not need to change the constants in Section 7.2. The rest of proofs  
 638 hold verbatim.

**C Remark on the volume of  $\mathcal{S}$**

► **Remark 35.** Because of symmetry the largest volume  $\mathcal{S}$  can attain is when both delimiting hyperplanes are equidistant to the center of  $B^d(r)$ . The volume of  $\mathcal{S}$  is given by the integral

$$r^d \int_{-\rho_1}^{\rho_1} \text{vol} \left( B_{d-1} \left( \sqrt{1-h^2} \right) \right) dh = \frac{\pi^{\frac{d-1}{2}}}{\Gamma(\frac{d+1}{2})} r^d \int_{-\rho_1}^{\rho_1} \left( \sqrt{1-h^2} \right)^{d-1} dh,$$

where  $B_{d-1}(r)$  denotes the ball on dimension  $d-1$  with radius  $r$  and  $\Gamma$  denotes the Euler gamma function. This integral can be expressed using special functions such as the hypergeometric function or beta functions. This gives an explicit value for  $\bar{\rho}_1$ .

**D Notation**

In the following table we give an overview of the notation used in this paper and compare it to Whitney’s notation.

Notation	definition	Whitney’s notation (if relevant)
$\mathcal{M}$	The manifold	$M$
$T\mathcal{M}, T_p\mathcal{M}$	The tangent bundle and the tangent space at $p$	$P_p$
$N\mathcal{M}, N_p\mathcal{M}$	The normal bundle and normal space at $p$	
$N_{\leq k}$	An upper bound on the total number of faces of dimension less or equal to $k$ that contain a given vertex.	Whitney does not distinguish dimensions and uses $N$ as an upper bound. (no value given)
$\text{rch}(\mathcal{M})$	The reach to the manifold $\mathcal{M}$	
$\mathcal{S}$	Slab between two hyperplanes intersected with a ball	$Q'$
$\mathcal{T}$	The ambient Coxeter triangulation of type $\tilde{A}$	$L$ is the ambient triangulation, but is not a Coxeter triangulation
$\tilde{\mathcal{T}}$	Perturbed ambient triangulation	$L^*$
$v_i$	Vertices of $\mathcal{T}$	$p_i$
$v_i^*$	Vertices of $\tilde{\mathcal{T}}$	$p_i^*$
$L(\cdot)$	Longest edge length	$\delta$ is the longest edge length of the ambient triangulation $L$
$U(X, r)$	A neighbourhood of radius $r$ of a set $X$	$U_r(X)$
$\bar{\rho}_1$	Volume fraction of the part of a ball inside a slab	$\rho_1$
$\rho_1$	Lower bound on $\bar{\rho}_1$ , see (4)	
$\delta$	Protection	
$\mu$	Separation as in an $(\epsilon, \mu)$ -net (the shortest edge length in $\mathcal{T}$ for Coxeter triangulations)	
$\epsilon$	The sampling density as in an $(\epsilon, \mu)$ -net (the circumradius of the simplices in the Coxeter triangulation)	
$\mu_0$	The normalized separation, that is $\mu = \mu_0 \epsilon$	

668	$A_i$	Affine subspaces	$P, P'$ and $Q$
669	$L(K)$	For any complex $K$ , $L(K)$ denotes the longest edge length in $K$	
670	$L$	$L = L(\mathcal{T})$	
671	$\tilde{L}$	$\tilde{L} = L(\tilde{\mathcal{T}})$	
672	$\tilde{c}L$	Perturbation radius of the vertices of $\mathcal{T}$	$\rho$
673	$\tilde{c}$	Normalized perturbation radius	$\rho^*$
674	$\tau, \sigma$	Simplices. We have tried to reserve $\tau$ for $\mathcal{T}$ or $\tilde{\mathcal{T}}$ and $\sigma$ for $K$ . However for arbitrary simplices (such as in Appendix A) we use arbitrary choices. Subscripts are used for indices and superscripts for the dimension.	Same
675	$t(\sigma)$	Thickness of $\sigma$	
676	aff	The affine hull	
677	$n$	Dimension of $\mathcal{M}$	$n$
678	$d$	Ambient dimension ( $\mathbb{R}^d$ )	$m$
679	$d(\cdot, \cdot)$	Euclidean distance between sets	
680	$d_{\mathcal{M}}(\cdot, \cdot)$	Distance on $\mathcal{M}$	
681	$\lambda$	barycentric coordinates	
682	$K$	Triangulation of $\mathcal{M}$	$K$
683	$B^d(c, r)$	A ball with in $\mathbb{R}^d$ of dimension with centre $c$ and radius $r$ , if we do not need to emphasize the centre or radius or they are to be determined, these are suppressed from the notation	$U_r(c)$
684	$B_{T_p\mathcal{M}}(c, r)$	A ball in $T_p\mathcal{M}$ , using the same conventions as for $B^d(c, r)$	
685	$\mathring{C}(T_p\mathcal{M}, r_1, r_2)$	Open cylinder given by all points that project orthogonally onto an open ball of radius $r_1$ in $T_p\mathcal{M}$ and whose distance to this ball is at most $r_2$	
686	$\pi_{\mathcal{M}}$	Closest point projection on $\mathcal{M}$	$\pi^*$
687	$\pi_{T_p\mathcal{M}}$	Orthogonal projection on the tangent spaces $T_p\mathcal{M}$	
688	$\pi_p^{-1}$	See Definition 4	
689	$\pi_{\text{aff}(\tau_k^{d-n}) \rightarrow N_p\mathcal{M}} = \pi_{\tau_k^{d-n}}$	The orthogonal projection map from the affine hull $\text{aff}(\tau_k^{d-n})$ to $N_p\mathcal{M}$ .	
690	$N_{v(\tau)}(e_i)$	See (20)	
691	$\mathcal{N}_{\bar{p}}$	The 'normal' space of $K$ at $\bar{p}$ , that is $\text{span}(N_{\bar{p}}(e_i))$	

692 **Overview most important bounds**

693  $\alpha_1$  and  $\alpha_k$  have been defined by a recursion relation as follows

694 
$$\alpha_1 = \frac{4}{3}\rho_1\tilde{c} \qquad \frac{2}{3}\alpha_{k-1}\tilde{c}\rho_1 = \alpha_k, \tag{5}$$

695 and thus  $\alpha_k = \frac{2^{k+1}}{3^k}\rho_1^k\tilde{c}^k$ . In particular we have the bound

696 
$$\alpha_k \leq \frac{1}{18^k}. \tag{6}$$

697  $L$  satisfies

$$698 \quad \left(1 - \sqrt{1 - \left(\frac{6L(\mathcal{T})}{\text{rch}(\mathcal{M})}\right)^2}\right) \text{rch}(\mathcal{M}) = \frac{(\alpha_{d-n})^{4+2n}}{6(n+1)^2} \zeta^{2n} L \quad (8)$$

699 or equivalently

$$700 \quad \frac{L}{\text{rch}(\mathcal{M})} = \frac{2 \frac{(\alpha_{d-n})^{4+2n}}{6(n+1)^2} \zeta^{2n}}{\left(\frac{(\alpha_{d-n})^{4+2n}}{6(n+1)^2} \zeta^{2n}\right)^2 + 6^2}, \quad (9)$$

701 with

$$702 \quad \zeta = \frac{8}{15\sqrt{d} \binom{d}{d-n} \cdot (1 + 2\tilde{c})} \left(1 - \frac{8\tilde{c}}{t(\mathcal{T})^2}\right) t(\mathcal{T}). \quad (7)$$

703 We often use

$$704 \quad \frac{L}{\text{rch}(\mathcal{M})} < \frac{(\alpha_{d-n})^{4+2n}}{54(n+1)^2} \zeta^n < \frac{(\alpha_{d-n})^2}{54}, \quad \frac{(\alpha_{d-n})^{4+2n}}{6(n+1)^2} \zeta^{2n} < \frac{(\alpha_{d-n})^2}{3} \leq \frac{\alpha_{d-n}}{3}. \quad (10)$$

705 The perturbation radius  $\tilde{c}$  satisfies

$$706 \quad |v_i - \tilde{v}_i| \leq \tilde{c}L = \min \left\{ \frac{t(\mathcal{T})\mu_0}{18d} \delta, \frac{1}{24} t(\mathcal{T})^2 L \right\}, \quad (14)$$

707 from which it follows that

$$708 \quad \tilde{c} \leq \frac{1}{24}. \quad (15)$$

709 **E Proofs**

710 **Proof of Lemma 3.** Apart from Lemma 2, we'll be using the following results from [10]:  
 711 For a minimizing geodesic  $\gamma$  on  $\mathcal{M}$  with length  $\ell$  parametrized by arc length, with  $\gamma(0) = p$   
 712 and  $\gamma(\ell) = q$

$$713 \quad \angle \dot{\gamma}(0) \dot{\gamma}(t) \leq \frac{t}{\text{rch}(\mathcal{M})}. \quad (24)$$

714 If we also write  $v_p = \dot{\gamma}(0)$  we have that

$$\begin{aligned} 715 \quad \langle \gamma(\ell), v_p \rangle &= \int_0^\ell \frac{d}{dt} (\langle \gamma(t), v_p \rangle) dt \\ 716 \quad &= \int_0^\ell \langle \dot{\gamma}(t), t_0 \rangle dt \\ 717 \quad &\geq \int_0^\ell \cos\left(\frac{t}{\text{rch}(\mathcal{M})}\right) dt \quad (\text{using (24)}) \\ 718 \quad &= \text{rch}(\mathcal{M}) \sin\left(\frac{\ell}{\text{rch}(\mathcal{M})}\right) \\ 719 \quad &\geq \text{rch}(\mathcal{M}) \sin(\angle(T_p\mathcal{M}, T_q\mathcal{M})), \quad (\text{using Lemma 2}) \end{aligned}$$

720 as long as  $\ell < \frac{1}{2} \text{rch}(\mathcal{M})\pi$ . Because  $v_p \in T_p\mathcal{M}$  and  $\gamma(\ell) = q$  we have that

$$721 \quad |p - \pi_{T_p\mathcal{M}}(q)| \geq \text{rch}(\mathcal{M}) \sin(\angle(T_p\mathcal{M}, T_q\mathcal{M})). \quad (25)$$

722 This means in particular that for all  $q$  such that  $|p - \pi_{T_p \mathcal{M}}(q)| < \text{rch}(\mathcal{M})$  and  $|q - \pi_{T_q \mathcal{M}}(q)| \leq$   
 723  $\text{rch}(\mathcal{M})$  the angle between  $T_p \mathcal{M}$  and  $T_q \mathcal{M}$  is less than 90 degrees. Note that the condition  
 724 on  $\ell$  mentioned above is satisfied by a combination of Theorem 1 and Lemma 11 of [10]. ◀

725 **Proof of Claim 10.** Choudhary et al. [13, Appendix B] provide explicit values of all the  
 726 quantities mentioned in Corollary 9 for a Coxeter triangulation of type  $\tilde{A}$ , with the exception  
 727 of  $\mu$ , which can be easily derived from a more general result. If we fix the scale (which in  
 728 [13] we did by a convenient choice of coordinates for the vertices), they are

$$\begin{aligned}
 729 \quad L(\sigma) &= \begin{cases} \frac{\sqrt{d+1}}{2} & \text{if } d \text{ is odd,} \\ \frac{1}{2} \sqrt{\frac{d(d+2)}{d+1}} & \text{if } d \text{ is even} \end{cases} & t(\sigma) &= \begin{cases} \sqrt{\frac{2}{d}} & \text{if } d \text{ is odd,} \\ \sqrt{\frac{2(d+1)}{d(d+2)}} & \text{if } d \text{ is even} \end{cases} \\
 730 \quad \epsilon &= \sqrt{\frac{d(d+2)}{12(d+1)}} & \delta(\sigma) &= \frac{\sqrt{d^2 + 2d + 24} - \sqrt{d^2 + 2d}}{\sqrt{12(d+1)}}. \quad (26)
 \end{aligned}$$

731 The value of  $\mu$  easily follows from the general expression of edge lengths (see [13, Ap-  
 732 pendix B,  $\tilde{A}_d$ , item 5]) and is equal to  $\mu = \sqrt{\frac{d}{d+1}}$ . From (26), we get that  $\mu_0 = \frac{\mu}{\epsilon} = \sqrt{\frac{12}{d+2}}$ .  
 733 The bound in (2) is therefore

$$\begin{aligned}
 734 \quad \tilde{c} &\leq \frac{t(\sigma)\mu_0}{18d} \frac{\delta}{L} = \begin{cases} \frac{\sqrt{2} \sqrt{d^2 + 2d + 24} - \sqrt{d^2 + 2d}}{9d^{3/2} \sqrt{d+2}(d+1)} & \text{if } d \text{ is odd,} \\ \frac{\sqrt{2(d+1)} \sqrt{d^2 + 2d + 24} - \sqrt{d^2 + 2d}}{9d^2 (d+2)^{3/2}} & \text{if } d \text{ is even.} \end{cases} \\
 735 &\leq \sqrt{2} \frac{\sqrt{d^2 + 2d + 24} - \sqrt{d^2 + 2d}}{9d^{3/2} \sqrt{d+2}(d+1)} \sim \frac{\sqrt{32}}{3d^4},
 \end{aligned}$$

736 where we used that  $\sqrt{1+x} \simeq 1 + \frac{1}{2}x$  if  $x$  is close to zero. ◀

737 **Proof of lemma 12.** We first notice that the barycentre  $c_b$  of a simplex  $\sigma^j$  is at least a dis-  
 738 tance  $\min \text{alt}(\sigma^j)/(j+1)$  removed from the faces of the simplex. This means that the ball in  
 739  $\text{aff}(\sigma^j)$  centred on  $c$  with radius  $\min \text{alt}(\sigma^j)/(j+1)$ , denoted by  $B_{\text{aff}(\sigma^j)}(c, \min \text{alt}(\sigma^j)/(j+1))$ ,  
 740 is contained in  $\sigma^j$ . We now consider any line segment  $\ell$  connecting a pair of anti-  
 741 podal points of  $\partial B_{\text{aff}(\sigma^j)}(c, \min \text{alt}(\sigma^j)/(j+1))$ . This line segment is contained in a  $d_{\max}$   
 742 neighbourhood of  $A_0$  and thus

$$743 \quad \sin \angle(\ell, A_0) \leq \frac{(j+1) d_{\max}}{\min \text{alt}(\sigma)}.$$

744 The result now follows, because  $\ell$  is arbitrarily chosen. ◀

745 **Proof of Claim 15.** Theorem 3 [24] gives us that for  $d \geq 2$  and  $1 \leq j \leq d-1$

$$746 \quad \frac{1}{2}(j^2 + j + 2)j^{d-j-1} - 1 \leq S(d, j) \leq \frac{1}{2} \binom{d}{j} j^{d-j}.$$

747 Furthermore, Stirlings theorem and the binomial theorem give that  $j! \sim j^j$  and  $\sum_{j=0}^k \binom{d}{j} \lesssim$   
 748  $d^k$ , respectively. We now see that

$$749 \quad N_{\leq k} = 2 + \sum_{j=1}^k j! S(d+1, j) \lesssim \sum_{j=1}^k j! \binom{d+1}{j} j^{d+1-j} \lesssim k^d \sum_{j=1}^k \binom{d}{j} \lesssim k^d d^k.$$

750 It is clear that if  $k$  is much smaller than  $d$  that then  $k^d$  dominates. ◀

751 **Proof of Lemma 16.** We can bound the volume of the slab  $\mathcal{S}$  by the cylinder with base  
 752  $B_{d-1}(r)$  and height  $2\rho_1 r$ , that is

$$753 \quad 2\rho_1 r^d \frac{\pi^{\frac{d-1}{2}}}{\Gamma(\frac{d+1}{2})}.$$

754 This means that

$$\begin{aligned} 755 \quad \frac{\text{vol}(\mathcal{S})}{\text{vol}(B^d(r))} &< \frac{2\rho_1 r \text{vol}(B_{d-1}(r))}{\text{vol}(B^d(r))} \\ 756 \quad &= \frac{2\rho_1 \frac{\pi^{\frac{d-1}{2}}}{\Gamma(\frac{d-1}{2}+1)}}{\frac{\pi^{\frac{d}{2}}}{\Gamma(\frac{d}{2}+1)}} \\ 757 \quad &= \frac{2\rho_1 \Gamma(\frac{d}{2}+1)}{\sqrt{\pi} \Gamma(\frac{d-1}{2}+1)} \\ 758 \quad &= \begin{cases} \frac{\pi(2k)!}{2^{2k-1}(k!)^2} \rho_1 & \text{if } d = 2k \\ \frac{2^{2k+1} k!(k-1)!}{(2k)!} \rho_1 & \text{if } d = 2k - 1. \end{cases} \end{aligned}$$

759 using the standard formulae for the volume of the ball, see for example [16, page 622]. Note  
 760 that the inequality is strict because  $\rho_1 > 0$ . We see that therefore  $\rho_1$  may be chosen to be

$$761 \quad \rho_1 = \begin{cases} \frac{2^{2k-2}(k!)^2}{\pi(2k)! N_{\leq d-n-1}} & \text{if } d = 2k \\ \frac{(2k)!}{2^{2k+2} k!(k-1)! N_{\leq d-n-1}} & \text{if } d = 2k - 1. \end{cases} \quad (4)$$

762 From Wendel's bound on the ratio of Gamma functions [25], we immediately see that for a  
 763 fixed constant  $a$ ,

$$764 \quad \frac{\Gamma(x+a)}{\Gamma(x)} \sim x^a.$$

765 This means that

$$766 \quad \frac{2\rho_1 \Gamma(\frac{d}{2}+1)}{\sqrt{\pi} \Gamma(\frac{d-1}{2}+1)} \sim \frac{2\rho(\frac{d}{2}+\frac{1}{2})^{1/2}}{\sqrt{\pi}} \sim \sqrt{d}.$$

767 We now see that

$$768 \quad \rho_1 \sim \frac{1}{\sqrt{d} N_{\leq d-n-1}}.$$

769 ◀

770 **Proof of Claim 18.** Because we assume that the perturbation is sufficiently small compared  
 771 to the protection, as given in the first condition of (14), (2) is satisfied and  $\tilde{\mathcal{T}}$  will have exactly  
 772 the same combinatorial structure as  $\mathcal{T}$ .

773 By the third condition of (14) we have a lower bound on the quality of the simplices. To  
 774 be precise, we have that for any simplex  $\tau$  in  $\tilde{\mathcal{T}}$

$$775 \quad t(\tau) \geq \frac{4}{5\sqrt{d}} \left(1 - \frac{8\tilde{c}}{t(\mathcal{T})^2}\right) t(\mathcal{T}), \quad (13)$$

776 as a consequence of Lemma 11, the fact that if you perturb the vertices by  $\tilde{c}L$  the edge  
 777 lengths are perturbed  $2\tilde{c}$  (that is  $2\tilde{c} = c_0$ ) and the fact that if  $\sigma \subset \tau$ , then  $t(\sigma) \geq t(\tau)$ . So  
 778 we have established (13). ◀



779 **Proof of Claim 19.** The argument is volumetric. Let us first introduce the notation  $U(X, r)$   
 780 for the set of all points  $x \in \mathbb{R}^d$  such that  $d(x, X) \leq r$ , where  $X$  is any subset of  $\mathbb{R}^d$ . By  
 781 definition of  $\rho_1$ , see 'Balls and exclusion volumes' in Section 5.1, and because the dimension  
 782 of  $\text{span}(\tau'_j, T_p\mathcal{M})$  is at most  $d - 1$ , we have that

$$783 \quad \text{vol}(B(v_i, \tilde{c}L) \cap U(\text{span}(\tau'_j, T_p\mathcal{M}), \rho_1\tilde{c}L)) \leq \frac{\text{vol}(B^d(r))}{2N_{\leq d-n-1}}.$$

784 It now follows that

$$\begin{aligned} 785 \quad & \text{vol} \left( B(v_i, \tilde{c}L) \setminus \left( \bigcup_{1 \leq j \leq \nu} U(\text{span}(\tau'_j, T_p\mathcal{M}), \rho_1\tilde{c}L) \right) \right) \\ 786 \quad & \geq \text{vol}(B(v_i, \tilde{c}L)) - \sum_{0 \leq j \leq \nu} \text{vol}(B(v_i, \tilde{c}L) \cap U(\text{span}(\tau'_j, T_p\mathcal{M}), \rho_1\tilde{c}L)) \\ 787 \quad & > \text{vol}(B(v_i, \tilde{c}L)) - \sum_{0 \leq j \leq \nu} \frac{\text{vol}(B(v_i, \tilde{c}L))}{2N_{\leq d-n-1}} \\ 788 \quad & = B(v_i, \tilde{c}L) \left( 1 - \frac{\nu + 1}{2N_{\leq d-n-1}} \right) \\ 789 \quad & \geq \frac{1}{2} B(v_i, \tilde{c}L), \end{aligned}$$

790 where we used that  $\nu \leq N_{\leq d-n-1}$  in the last line, by definition, as mentioned in the de-  
 791 scription of Case 2. Because the volume is positive we know there exists a point  $\tilde{v}_i$  that  
 792 satisfies

$$793 \quad d(\tilde{v}_i, \text{span}(\tau'_j, T_p\mathcal{M})) > \rho_1\tilde{c}L, \tag{27}$$

794 for all  $1 \leq j \leq \nu$ . ◀

796 **Proof of Claim 20.** We first make use of the induction<sup>2</sup> hypothesis  $d(\tau'_j, \mathcal{M}) > \alpha_{k-1}L$  to  
 797 find a bound on the distance from  $\tau'_j$  to the tangent space  $T_p\mathcal{M}$ , then bound the distance  
 798 from  $\tilde{v}_i * \tau'_j = \tau_j$  to  $T_p\mathcal{M}$  based on this. For this argument to work, we have to assume that  
 799  $\tau'_j$  is not the empty set, that is  $j \neq 0$ . This case is handled separately at the end.

800 Because  $d(\tau'_j, \mathcal{M}) > \alpha_{k-1}L$  and the ball in the tangent space  $B_{T_p\mathcal{M}}(p, r)$  centred on  $p$  of  
 801 radius  $6L = r$ , satisfies

$$802 \quad B_{T_p\mathcal{M}}(p, r) \subset U \left( \mathcal{M}, \left( 1 - \sqrt{1 - \left( \frac{r}{\text{rch}(\mathcal{M})} \right)^2} \right) \text{rch}(\mathcal{M}) \right).$$

803 Thanks to Lemma 6, we have that

$$804 \quad d(\tau'_j, B_{T_p\mathcal{M}}(p, r)) > \alpha_{k-1}L - \left( 1 - \sqrt{1 - \left( \frac{r}{\text{rch}(\mathcal{M})} \right)^2} \right) \text{rch}(\mathcal{M}).$$

---

795 <sup>2</sup> In particular  $\tau'_j \subset \tilde{\tau}_i$ .

805 This can be simplified:

$$\begin{aligned}
 806 \quad & d(\tau'_j, B_{T_p \mathcal{M}}(p, r)) \\
 807 \quad & > \alpha_{k-1}L - \left(1 - \sqrt{1 - \left(\frac{r}{\text{rch}(\mathcal{M})}\right)^2}\right) \text{rch}(\mathcal{M}) \\
 808 \quad & > \alpha_{k-1}L - \frac{(\alpha_{d-n})^{4+2n}}{6(n+1)^2} \zeta^{2n} L \quad (\text{using (8)}) \\
 809 \quad & > \alpha_{k-1}L - \frac{1}{3} \alpha_{d-n} L \quad (\text{using (10)}) \\
 810 \quad & \geq \frac{2}{3} \alpha_{k-1} L. \quad (\text{because } \alpha_{k-1} > \alpha_k) \\
 811 \quad & \tag{28}
 \end{aligned}$$

812 Because  $d(v_i, p) < \frac{3}{2}L$  and  $\tilde{L} < L + 2\tilde{c}L$ , and  $\tilde{c} < \frac{1}{24}$ , see (15), we have the very course  
 813 bound that

$$814 \quad d(\tau'_j, p) \leq 4L, \tag{29}$$

815 by the triangle inequality. We thus find that

$$816 \quad d(\tau'_j, T_p \mathcal{M} \setminus B_{T_p \mathcal{M}}(p, r)) > 2L.$$

817 This means that (28) holds for the entire tangent space, that is,

$$818 \quad d(\tau'_j, T_p \mathcal{M}) > \frac{2}{3} \alpha_{k-1} L. \tag{30}$$

819 Lemma 31, with  $A_1 = T_p \mathcal{M}$  and  $A_2 = \text{span}(\tau'_j, T_p \mathcal{M})$ , now gives

$$820 \quad d(\tau_j, T_p \mathcal{M}) \geq \frac{d(\tau'_j, T_p \mathcal{M})d(v_i, \text{span}(\tau'_j, T_p \mathcal{M}))}{L + 2\tilde{c}L}.$$

821 This can again be simplified

$$\begin{aligned}
 822 \quad & d(\tau_j, T_p \mathcal{M}) \geq \frac{d(\tau'_j, T_p \mathcal{M})d(v_i, \text{span}(\tau'_j, T_p \mathcal{M}))}{L + 2\tilde{c}L} \\
 823 \quad & > \frac{\left(\frac{2}{3} \alpha_{k-1} L\right) \rho_1 \tilde{c} L}{L + 2\tilde{c}L} \quad (\text{thanks to (30) and (17)}) \\
 824 \quad & > \frac{\frac{2}{3} L}{\frac{4}{3} L} \alpha_{k-1} \rho_1 \tilde{c} L \quad (\text{because } \tilde{c} \leq \frac{1}{24}) \\
 825 \quad & = \frac{4}{3} \alpha_k L. \quad (\text{using the relation (5) for } \alpha_k) \\
 826 \quad & \tag{31}
 \end{aligned}$$

827 Similarly to (29), we have that

$$828 \quad d(\tau_j, p) \leq 4L < 6L.$$

829 We can go from the distance from  $\tau_j$  to the tangent space, as given in (31), to the distance  
 830 to the manifold as follows. Because of Lemma 5 we can localize the results and Lemma 6

00:26 An elementary and quantified version of Whitney's triangulation method

831 allows us to estimate the difference in distance to the manifold and the tangent space. This  
832 gives

$$833 \quad d(\tau_j, \mathcal{M}) > \frac{4}{3}\alpha_k L - \left(1 - \sqrt{1 - \left(\frac{6L}{\text{rch}(\mathcal{M})}\right)^2}\right) \text{rch}(\mathcal{M}).$$

834 This can be again simplified

$$\begin{aligned} 835 \quad d(\tau_j, \mathcal{M}) &> \frac{4}{3}\alpha_k L - \left(1 - \sqrt{1 - \left(\frac{6L}{\text{rch}(\mathcal{M})}\right)^2}\right) \text{rch}(\mathcal{M}) \\ 836 \quad &> \frac{4}{3}\alpha_k L - \frac{1}{3}\alpha_{d-n} L && \text{(using (8) and (10))} \\ 837 \quad &\geq \alpha_k L. && \text{(because } \alpha_k \geq \alpha_{d-n} \text{ if } k \leq d-n-1 \text{ by (5))} \end{aligned}$$

838 This completes the proof for the case where  $j \neq 0$  or  $\tau_j$  is non-empty.

839 For  $j = 0$ , (27) and Lemma 6 yield

$$840 \quad d(\tau_j, \mathcal{M}) > \rho_1 \tilde{c} L - \left(1 - \sqrt{1 - \left(\frac{6L}{\text{rch}(\mathcal{M})}\right)^2}\right) \text{rch}(\mathcal{M}).$$

841 We simplify

$$\begin{aligned} 842 \quad d(\tau_j, \mathcal{M}) &> \rho_1 \tilde{c} L - \left(1 - \sqrt{1 - \left(\frac{6L}{\text{rch}(\mathcal{M})}\right)^2}\right) \text{rch}(\mathcal{M}). \\ 843 \quad &> \rho_1 \tilde{c} L - \frac{1}{3}\alpha_{d-n} L && \text{(using (8) and (10))} \\ 844 \quad &> \alpha_1 L. && \text{(by definition of (5))} \end{aligned}$$

845

846 The following proof differs from Whitney's proof.

847 **Proof of Lemma 21.** Because  $\tau^k \subset B(p, 6L)$ , the point in  $T_p \mathcal{M}$  that is closest to  $\tau$  lies in  
848  $T_p \mathcal{M} \cap B(p, 6L) = B_{T_p \mathcal{M}}(p, 6L)$ . We now see that

$$\begin{aligned} 849 \quad d(\tau^k, T_p \mathcal{M}) &\geq d(\tau^k, B_{T_p \mathcal{M}}(p, 6L)) && \text{(first sentence of the proof)} \\ &> d(\tau^k, \mathcal{M}) - \left(1 - \sqrt{1 - \left(\frac{6L}{\text{rch}(\mathcal{M})}\right)^2}\right) \text{rch}(\mathcal{M}) && \text{(Lemma 6)} \\ 850 \quad &> \alpha_k L - \frac{1}{3}\alpha_{d-n} L, && \text{(} d(\tau^k, \mathcal{M}) > \alpha_k L \text{ and (10))} \\ 851 \quad &> \frac{2}{3}\alpha_k L, && \text{(} \alpha_k \geq \alpha_{d-n} \text{ for } k \leq d-n \text{)} \\ 852 \end{aligned}$$

853 which completes the proof. ◀

854 **Proof of Lemma 22.** Let  $\bar{p} \in \mathcal{M} \cap \tau^k$ . Lemma 3 (and (8), (10)) gives us that  $\bar{p} \in \pi_p^{-1}$   
855  $(B_{T_p \mathcal{M}}(p, 6L))$ , where we use the notation of Definition 4. Lemma 6 gives that

$$856 \quad d(\bar{p}, T_p \mathcal{M}) \leq \left(1 - \sqrt{1 - \left(\frac{6L}{\text{rch}(\mathcal{M})}\right)^2}\right) \text{rch}(\mathcal{M}) < \frac{1}{3}\alpha_{d-n} L.$$

857 Let  $\check{\tau} \subset \tau^k$  be the face of smallest dimension such that  $d(\check{\tau}, T_p\mathcal{M}) \leq \frac{2}{3}\alpha_{d-n}L$ . This face  
 858 exists thanks to the triangle inequality. By Lemma 21 we have the  $\dim(\check{\tau}) \geq d - n$ . Lemma  
 859 30 implies that  $\check{\tau}$  intersects  $T_p\mathcal{M}$ . The reason for this is the following;  $\check{\tau}$  is the simplex of the  
 860 smallest dimension such that  $d(\check{\tau}, T_p\mathcal{M}) \leq \frac{2}{3}\alpha_k L$  meaning in particular that  $d(\check{\tau}, T_p\mathcal{M}) <$   
 861  $d(\partial\check{\tau}, T_p\mathcal{M})$ . Because  $\check{\tau}$  is a face of  $\tau^k$ , clearly  $T_p\mathcal{M}$  intersects  $\tau^k$ . ◀

862 **Proof of Lemma 23.** This is an immediate consequence of Lemma 30, (14), and the previ-  
 863 ous lemmas. ◀

864 **Proof of Lemma 24.** Let  $\check{\tau}$  be a face of smallest dimension of  $\tau^k$  such that  $d(\check{\tau}, T_p\mathcal{M}) \leq$   
 865  $\frac{2}{3}\alpha_n L$ . Now Lemma 30 and Lemma 22 give that  $\check{\tau}$  and  $T_p\mathcal{M}$  have a unique point  $\bar{p}$  in  
 866 common and the dimension of  $\check{\tau}$  is  $d - n$ .

867 Thanks to Lemma 3,  $\mathcal{M}$  can be written as the graph of a function  $f$ , in a neighbourhood  
 868 of at most size  $\text{rch}(\mathcal{M})$ . We note that  $f : T_p\mathcal{M} \simeq \mathbb{R}^n \rightarrow N_p\mathcal{M} \simeq \mathbb{R}^{d-n}$ , where here we  
 869 really think of the tangent and normal spaces as embedded in  $\mathbb{R}^d$ . Using the identification  
 870 of  $T_p\mathcal{M}$  with  $\mathbb{R}^n$ , we now define

$$871 \quad F : \mathbb{R} \times \mathbb{R}^n \rightarrow \mathbb{R}^d : (\lambda, x) \mapsto (x, \lambda f(x)).$$

872 Note that  $F(0, \cdot)$  gives a parametrization of  $T_p\mathcal{M}$ . Similarly, we can define  $G : \mathbb{R}^{d-n} \rightarrow \mathbb{R}^d$   
 873 to be a linear (orthonormal) parametrization of  $\text{aff}(\check{\tau})$ . We now consider the difference of  
 874 the two functions  $F - G : \mathbb{R} \times \mathbb{R}^n \times \mathbb{R}^{d-n} = \mathbb{R} \times \mathbb{R}^d \rightarrow \mathbb{R}^d$ . Thanks to Lemma 23 we have  
 875 that

$$876 \quad \sin \angle(\text{aff}(\check{\tau}), T_p\mathcal{M}) \geq \frac{16}{10}\alpha_{d-n}.$$

877 Lemma 2, and (10) give that for any  $q \in B(p, 6L)$

$$878 \quad \sin \left( \frac{\angle(T_p\mathcal{M}, T_q\mathcal{M})}{2} \right) \leq \frac{6L}{2\text{rch}(\mathcal{M})} \leq \frac{6}{2} \cdot \frac{(\alpha_{d-n})^2}{54} = \frac{1}{18}(\alpha_{d-n})^2.$$

879 It is clear that this also gives an upper bound on the angle between  $T_p\mathcal{M}$  and the graph  
 880 of  $F(\lambda, \cdot)$  (denoted by  $\text{graph } F(\lambda, \cdot)$ ) for all  $\lambda \in [0, 1]$ , due to linearity of the inner product.  
 881 Because the upper bound on the angle between the tangent spaces is much smaller than the  
 882 lower bound on  $\angle(\text{aff}(\tau^k), T_p\mathcal{M})$ ,  $\text{aff}(\check{\tau})$  and  $T_q \text{graph } F(\lambda, \cdot)$  span  $\mathbb{R}^d$ , for any  $\lambda \in [0, 1]$  and  
 883  $q \in B(p, 6L)$ . The implicit function theorem and the fact that  $\check{\tau}$  and  $T_p\mathcal{M}$  have a unique  
 884 point  $\bar{p}$  in common now give that the intersection  $\bar{p}_\lambda$  between  $\text{graph } F(\lambda, \cdot) \cap B(p, 6L)$  and  
 885  $\text{aff}(\check{\tau})$  exists and is unique, for all  $\lambda \in [0, 1]$ .

886 We can now use Lemmas 3, 6, and 23, to bound  $|\bar{p} - \bar{p}_\lambda|$ . The distance from the manifold  
 887 to the tangent space (and thus the same holds for  $\text{graph } F(\lambda, \cdot)$ ) is bounded from above by

$$888 \quad \frac{(\alpha_{d-n})^{3+2n}}{3(n+1)} \zeta^{2n} L < \frac{1}{3}(\alpha_{d-n})^2 L,$$

889 due to (8), and (10), while  $\sin \angle(\text{aff}(\check{\tau}), T_p\mathcal{M}) \geq \frac{16}{10}\alpha_{d-n}$ , so

$$890 \quad |\bar{p} - \bar{p}_\lambda| \leq \frac{\frac{1}{3}(\alpha_{d-n})^2 L}{\frac{16}{10}\alpha_{d-n}} \leq \frac{1}{3}\alpha_{d-n}L.$$

891 This distance bound is smaller than the distance bound of  $\bar{p}$  to the boundary of  $\check{\tau}$ , due to  
 892 Lemma 21. This means that  $\bar{p}_\lambda \in \check{\tau}$ , and in particular that  $\mathcal{M}$  intersects  $\tau^k$ . ◀

893 **Proof of Lemma 25.** Take  $p \in \mathcal{M} \cap \tau$ . Let  $\check{\tau}^k$  be a face of the smallest dimension of  $\tau$ , with  
 894  $v_i \in \check{\tau}^k$ , that intersects  $T_p\mathcal{M}$ . Now assume that  $k > d - n$ . Let us write  $\check{\tau}^{k-1}$  for the face  
 895 of  $\check{\tau}^k$  opposite  $v_i$ . Because the dimension of  $\check{\tau}^k \cap T_p\mathcal{M}$  is at least 1, the intersection of  $T_p\mathcal{M}$   
 896 and  $\check{\tau}^{k-1}$  is non-empty.

897 Similarly to the first argument in the proof of Lemma 24, we see that  $T_p\mathcal{M}$  intersects  
 898 some  $(d - n)$ -face of  $\check{\tau}^{k-1}$ . Thanks to Lemma 23 the angle between this  $(d - n)$ -face and  
 899  $T_p\mathcal{M}$  is bounded from below. Due to Lemma 21 the intersection lies in the interior of the  
 900  $(d - n)$ -face. The angle bound and the fact that the intersection lies in the interior gives  
 901 that any simplex in  $\mathcal{T}$  that contains this  $(d - n)$ -face has points in the interior that lie in  
 902  $T_p\mathcal{M}$ . In particular the interior of  $\check{\tau}^k$  contains part of  $T_p\mathcal{M}$ . Because both the interior of  $\check{\tau}^k$   
 903 and  $\check{\tau}^{k-1}$  contain points of  $T_p\mathcal{M}$ , linearity gives that  $T_p\mathcal{M}$  must intersect  $\partial\check{\tau}^k \setminus \check{\tau}^{k-1}$ . From  
 904 this contradiction of the assumption, we conclude that  $k = d - n$ .

905 Lemma 24 finally says that  $\mathcal{M}$  intersects  $\check{\tau}^k$ , because  $T_p\mathcal{M}$  does.  $\blacktriangleleft$

906 **Proof of Lemma 26.** This inequality relies on estimates on the barycentric coordinates, and  
 907 Lemma 11. We first establish a bound on the barycentric coordinates of  $v(\tau_i^{d-n})$  for some  
 908  $(d - n)$ -dimensional simplex  $\tau_i^{d-n} \in \tilde{\mathcal{T}}$  that intersects  $\mathcal{M}$ . By Lemma 21,  $v(\tau_i^{d-n})$  lies at least  
 909 a distance  $\frac{2}{3}\alpha_{d-n-1}L$  from the boundary  $\partial\tau_i^{d-n}$  and the longest edge is at most  $L + 2\tilde{c}L$ .  
 910 This means that all the barycentric coordinates  $\lambda_l$  with respect to (the vertices of)  $\tau_i^{d-n}$  are  
 911 at least

$$912 \quad \lambda_l(\tau_i^{d-n}) > \frac{2}{3}\alpha_{d-n-1}\frac{L}{L + 2\tilde{c}L} = \frac{2}{3}\alpha_{d-n-1}\frac{1}{1 + 2\tilde{c}}. \quad (32)$$

913 Let  $\tau^d$  now be a top dimensional simplex in  $\tilde{\mathcal{T}}$  that intersects  $\mathcal{M}$ . Let  $\tau_1^{d-n}, \dots, \tau_j^{d-n}$  be  
 914 the faces of  $\tau^d$  that intersect  $\mathcal{M}$ . This means that  $d - n + 1$  barycentric coordinates with  
 915 respect to  $\tau^d$  of any  $v(\tau_i^{d-n})$  satisfy the bound (32), while the other  $n$  coordinates are zero.  
 916 This also means that for the barycentric coordinates with respect to  $\tau^d$  of

$$917 \quad v(\tau^k) = \frac{1}{j}(v(\tau_1^{d-n}) + \dots + v(\tau_j^{d-n})),$$

918 for  $k > d - n$ , we have that

919  $\blacksquare$   $k + 1$  of the coordinates  $\lambda_l$  satisfy

$$920 \quad \lambda_l > \frac{2}{3}\frac{1}{j}\frac{1}{1 + 2\tilde{c}}\alpha_{d-n-1}.$$

921  $\blacksquare$  The other  $d - k$  coordinates are zero.

922 Note that  $j \leq \binom{d}{d-n}$ . This means that

$$923 \quad d(v(\tau^k), \partial\tau^k) \geq \frac{2}{3\binom{d}{d-n} \cdot (1 + 2\tilde{c})}\alpha_{d-n-1} \min \text{alt}(\tau^d).$$

924 We now have

$$925 \quad d(v(\tau^k), \partial\tau^k) \geq \frac{2}{3\binom{d}{d-n} \cdot (1 + 2\tilde{c})}\alpha_{d-n-1}t(\tilde{\mathcal{T}})\tilde{L} \quad (\text{by definition of the thickness})$$

$$926 \quad \geq \frac{2}{3\binom{d}{d-n} \cdot (1 + 2\tilde{c})}\alpha_{d-n-1}\frac{4}{5\sqrt{d}}\left(1 - \frac{8\tilde{c}}{t(\mathcal{T})^2}\right)t(\mathcal{T})\tilde{L}$$

(by the estimate (13))

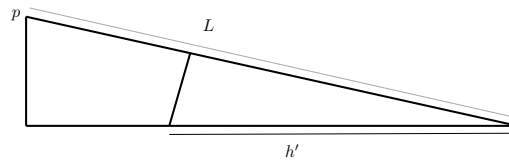
$$927 \quad \geq \frac{8}{15\sqrt{d}\binom{d}{d-n} \cdot (1 + 2\tilde{c})}\left(1 - \frac{8\tilde{c}}{t(\mathcal{T})^2}\right)\alpha_{d-n-1}t(\mathcal{T})\tilde{L}$$

928 Using this estimate and the fact that  $\sigma^n$  defined through a sequence  $\tau_0^{d-n} \subset \tau_1^{d-n+1} \subset \dots \subset$   
 929  $\tau_n^d$  we can give a lower bound on the minimal altitude of the simplex.

930 We are going to use the following easy observation on the minimal altitude simplices.  
 931 Suppose that:

- 932 ■ The simplex  $\sigma$  is the join of a point  $p$  and the simplex  $\sigma'$ .
- 933 ■  $d(p, \text{aff}(\sigma')) \geq d_{\min}$ .
- 934 ■  $\min \text{alt}(\sigma') \geq h'$ .
- 935 ■ The maximum edge length of  $\sigma$  is  $L(\sigma)$ .

937 Then the  $\min \text{alt}(\sigma) \geq \frac{h' d_{\min}}{L(\sigma)}$ , as can be established by simple trigonometric arguments, as illustrated in Figure 3



936 ■ **Figure 3** Both triangles are right angled.

938 This gives that  $\min \text{alt}(\sigma^n)$  with  $\sigma^n$  as in (18) is lower bounded as follows:  
 939

$$940 \quad \min \text{alt}(\sigma^n) > \left( \frac{8}{15\sqrt{d} \binom{d}{d-n} \cdot (1 + 2\tilde{c})} \left( 1 - \frac{8\tilde{c}}{t(\mathcal{T})^2} \right) \alpha_{d-n-1} t(\mathcal{T}) \right)^n \tilde{L}$$

$$941 \quad = \zeta^n (\alpha_{d-n-1})^n \tilde{L},$$

942 which completes the proof. ◀

943 **Proof of Lemma 27.** By Lemma 12 we have that

$$944 \quad \sin \angle(\text{aff}(\sigma^n), T_p \mathcal{M}) \leq \frac{(n+1) d_{\max}}{\min \text{alt}(\sigma^n)},$$

945 where  $d_{\max}$  denotes the maximum distance of the vertices of  $\sigma^n$  to  $T_p \mathcal{M}$ . Lemma 26 gives  
 946 us the following bound

$$947 \quad \min \text{alt}(\sigma^n) > (\alpha_{d-n-1})^n \zeta^n \tilde{L}.$$

948 Finally,  $d_{\max}$  is bounded thanks to (8). Combining these results yields

$$949 \quad \sin \angle(\text{aff}(\sigma^n), T_p \mathcal{M}) \leq \frac{(n+1) \frac{(\alpha_{d-n})^{4+2n}}{6(n+1)^2} \zeta^{2n} L}{(\alpha_{d-n-1})^n \zeta^n \tilde{L}}$$

$$950 \quad \leq \frac{(\alpha_{d-n})^{4+n}}{6(n+1)} \zeta^n.$$

(because  $\alpha_{d-n-1} < \alpha_{d-n}$ , and  $\tilde{L} \geq L$  because there are unperturbed simplices in  $\tilde{\mathcal{T}}$ )

951 ◀

952 **Proof of Lemma 28.** We first establish a bound on the angles between  $\mathcal{N}_{\tilde{p}}$  and  $\mathcal{N}_{\tilde{q}}$ . Lemma  
 953 23 gives that for each  $\tau^{d-n}$

$$954 \quad \sin \angle(\text{aff}(\tau^{d-n}), T_p \mathcal{M}) \geq \frac{16}{10} \alpha_{d-n},$$

955 so that

$$956 \quad \cos \angle(\pi_{\text{aff}(\tau^{d-n}) \rightarrow N_p \mathcal{M}}^{-1}(e_j), e_j) \geq \frac{16}{10} \alpha_{d-n},$$

957 with  $e_i$  a basis vector of  $N_p \mathcal{M}$  as in Section 7.1. This means that  $|\pi_{\text{aff}(\tau^{d-n}) \rightarrow N_p \mathcal{M}}^{-1}(e_j)| \leq$   
 958  $\frac{10}{16 \alpha_{d-n}}$  and as a consequence of this and the triangle inequality we find that  $|N_{v(\tau)}(e_j)|, |N_{\bar{p}'}(e_j)| \leq$   
 959  $\frac{10}{16 \alpha_{d-n}}$ , for any  $\bar{p}'$ . This in turn gives us that

$$960 \quad \angle(N_{\bar{p}'}(e_j), e_j) \leq \arccos \left( \frac{16}{10} \alpha_{d-n} \right). \quad (33)$$

961 The triangle inequality for angles (or points on the sphere) now implies that

$$962 \quad \angle(N_{\bar{p}}(e_j), N_{\bar{q}}(e_j)), \angle(N_{v(\tau_0^{d-n})}(e_j), N_{v(\tau_n^{d-n})}(e_j)) \leq 2 \arccos \left( \frac{16}{10} \alpha_{d-n} \right).$$

963 We can tighten this result for  $\angle(N_{\bar{p}}(e_j), N_{\bar{q}}(e_j))$  by the use of the barycentric coordin-  
 964 ates. We now consider the  $e_i$  component of both  $\lambda_0 N_{v(\tau_0^{d-n})}(e_i) + \dots + \lambda_n N_{v(\tau_n^{d-n})}(e_i)$   
 965 and  $\lambda'_0 N_{v(\tau_0^{d-n})}(e_i) + \dots + \lambda'_n N_{v(\tau_n^{d-n})}(e_i)$  is  $e_i$ , by construction. We are going to com-  
 966 pare this with the length of  $\lambda_0 N_{v(\tau_0^{d-n})}(e_i) + \dots + \lambda_n N_{v(\tau_n^{d-n})}(e_i)$  and  $\lambda'_0 N_{v(\tau_0^{d-n})}(e_i) +$   
 967  $\dots + \lambda'_n N_{v(\tau_n^{d-n})}(e_i)$ . For estimates on these lengths we need to introduce the following  
 968 notation:  $(N_{v(\tau_0^{d-n})}(e_i) \dots N_{v(\tau_n^{d-n})}(e_i))$  denotes the matrix whose columns are the vectors  
 969  $N_{v(\tau_0^{d-n})}(e_i), \dots, N_{v(\tau_n^{d-n})}(e_i)$ ,  $\|\cdot\|_2$  denotes the operator 2-norm, and  $\|\cdot\|_F$  the Frobenius  
 970 norm. With this notation we can now derive the following bound:

$$\begin{aligned} 971 \quad & |\lambda_0 N_{v(\tau_0^{d-n})}(e_i) + \dots + \lambda_n N_{v(\tau_n^{d-n})}(e_i) - (\lambda'_0 N_{v(\tau_0^{d-n})}(e_i) + \dots + \lambda'_n N_{v(\tau_n^{d-n})}(e_i))| \\ 972 \quad & = |(\lambda_0 - \lambda'_0) N_{v(\tau_0^{d-n})}(e_i) + \dots + (\lambda_n - \lambda'_n) N_{v(\tau_n^{d-n})}(e_i)| \\ 973 \quad & = \left| \left( N_{v(\tau_0^{d-n})}(e_i) \dots N_{v(\tau_n^{d-n})}(e_i) \right) \begin{pmatrix} \lambda_0 - \lambda'_0 \\ \vdots \\ \lambda_n - \lambda'_n \end{pmatrix} \right| \\ 974 \quad & \leq \| (N_{v(\tau_0^{d-n})}(e_i) \dots N_{v(\tau_n^{d-n})}(e_i)) \|_2 |\lambda - \lambda'| \\ 975 \quad & \leq \| (N_{v(\tau_0^{d-n})}(e_i) \dots N_{v(\tau_n^{d-n})}(e_i)) \|_F |\lambda - \lambda'| \quad (\text{because } \|\cdot\|_2 \leq \|\cdot\|_F) \\ 976 \quad & = \sqrt{|N_{v(\tau_0^{d-n})}(e_i)|^2 + \dots + |N_{v(\tau_n^{d-n})}(e_i)|^2} |\lambda - \lambda'| \\ 977 \quad & \leq \frac{10\sqrt{n+1}}{16 \alpha_{d-n}} |\lambda - \lambda'|. \end{aligned}$$

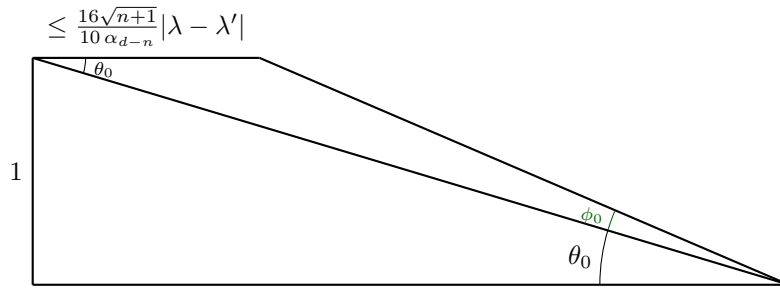
978 We now turn our attention to the triangle, with edges  $N_{\bar{p}}(e_j)$ ,  $N_{\bar{q}}(e_j)$ , and  $N_{\bar{p}}(e_j) - N_{\bar{q}}(e_j)$   
 979 as depicted in Figure 4. We apply the sine rule to this triangle and find

$$980 \quad \sin \angle(N_{\bar{p}}(e_j), N_{\bar{q}}(e_j)) \leq \sin \phi_0 = \frac{\frac{10\sqrt{n+1}}{16 \alpha_{d-n}} |\lambda - \lambda'| \frac{10}{16 \alpha_{d-n}}}{1} = \left( \frac{10}{16 \alpha_{d-n}} \right)^2 \sqrt{n+1} |\lambda - \lambda'|. \quad (34)$$

981 Note that this can be tightened at the cost of introducing extra square roots.

982 We now consider the triangle  $\bar{p}\bar{q}x$  and we want to estimate  $|\bar{p}x|$ , and  $|\bar{q}x|$ . This following  
 983 estimate will use:

984 ■ the sine rule



982 **Figure 4** The worst case for the angle between the vectors  $N_{\bar{p}}(e_j)$ , and  $N_{\bar{q}}(e_j)$ . We write  $\phi_0$  for  
 983 an upper bound on  $\angle(N_{\bar{p}}(e_j), N_{\bar{q}}(e_j))$ . Moreover  $\theta_0 \geq \arccos(\frac{16}{10}\alpha_{d-n})$ . The length or bound on the  
 984 length of two of the edges is also indicated in the figure.

- 988 ■ the fact that the distance between  $\bar{p}$  and  $\bar{q}$ , is at least  $|\lambda - \lambda'| \min \text{alt}(\sigma)/\sqrt{n}$ , thanks to
- 989 Lemma 5.12 of [7]
- 990 ■ Lemma 26 to bound  $\min \text{alt}(\sigma)$
- 991 ■ Equation (34), which gives a bound on the angle  $\angle\bar{p}\bar{q}$ , namely  $\phi_0$
- 992 ■ Lemma 27, gives that

$$993 \quad \angle(\text{aff}(\sigma^n)^\perp, N_p\mathcal{M}) \leq \arcsin\left(\frac{(\alpha_{d-n})^{4+n}}{6(n+1)}\zeta^n\right) \leq \arcsin\left(\frac{(\alpha_{d-n})^3}{3}\right), \quad (35)$$

994 where  $\text{aff}(\sigma^n)^\perp$  denotes the space perpendicular to  $\text{aff}(\sigma^n)$ . Because  $e_j \in N_p\mathcal{M}$ , combin-  
 995 ing this with Lemma 23 and the triangle inequality for angles yields

$$996 \quad \begin{aligned} \angle(N_{\bar{p}'}(e_j), \text{aff}(\sigma^n)^\perp) &\leq \angle(N_{\bar{p}'}(e_j), e_j) + \angle(N_p\mathcal{M}, \text{aff}(\sigma^n)^\perp) \\ 997 \quad &\leq \arccos\left(\frac{16}{10}\alpha_{d-n}\right) + \arcsin\left(\frac{(\alpha_{d-n})^3}{3}\right). \end{aligned} \quad (36)$$

998 We need a lower bound on  $\sin(\angle\bar{p}\bar{q}x)$  and  $\sin(\angle\bar{q}\bar{p}x)$ , that is

$$999 \quad \sin \angle(N_{\bar{p}'}(e_j), \text{aff}(\sigma^n)) = \cos \angle(N_{\bar{p}'}(e_j), \text{aff}(\sigma^n)^\perp).$$

1000 We also remind ourselves of the trigonometric identity

$$1001 \quad \cos(\arccos(a) + \arcsin(b)) = a\sqrt{1-b^2} - b\sqrt{1-a^2}.$$

1002 Using (36) now gives

$$1003 \quad \begin{aligned} \sin \angle(N_{\bar{p}'}(e_j), \text{aff}(\sigma^n)) &\geq \cos\left(\arccos\left(\frac{16}{10}\alpha_{d-n}\right) + \arcsin\left(\frac{(\alpha_{d-n})^3}{3}\right)\right) \\ 1004 \quad &= \left(\frac{16}{10}\alpha_{d-n}\right)\sqrt{1 - \frac{(\alpha_{d-n})^6}{3^2}} - \frac{(\alpha_{d-n})^3}{3}\sqrt{1 - \left(\frac{16}{10}\alpha_{d-n}\right)^2} \\ 1005 \quad &\geq \frac{16}{10}\alpha_{d-n} - \left(\frac{16}{10}\alpha_{d-n}\right)\frac{(\alpha_{d-n})^6}{3^2} - \frac{(\alpha_{d-n})^3}{3} \\ 1006 \quad &\geq \frac{16}{10}\alpha_{d-n} - \frac{5(\alpha_{d-n})^3}{9} \\ 1007 \quad &\geq \alpha_{d-n}. \end{aligned} \quad (37)$$



1008 The considerations we summed up yield:

$$\begin{aligned}
 1009 \quad |\bar{p}x|, |\bar{q}x| &\geq \frac{(|\lambda - \lambda'| \min \text{alt}(\sigma) / \sqrt{n}) \alpha_{d-n}}{\left(\frac{10}{16\alpha_{d-n}}\right)^2 \sqrt{n+1} |\lambda - \lambda'|} \\
 1010 &\geq \frac{\min \text{alt}(\sigma) \alpha_{d-n} \left(\frac{16}{10}\alpha_{d-n}\right)^2}{n+1} \\
 1011 &\geq \frac{\alpha_{d-n} \left(\frac{16}{10}\alpha_{d-n}\right)^2}{n+1} (\zeta \alpha_{d-n-1})^n \tilde{L}
 \end{aligned}$$

1012 Using (37) again yields that the distance from  $x$  to  $\text{aff}(\sigma^n)$  is bounded from below by

$$1013 \quad d(x, \text{aff}(\sigma^n)) \geq \frac{(\alpha_{d-n})^2 \left(\frac{16}{10}\alpha_{d-n}\right)^2}{n+1} (\zeta \alpha_{d-n-1})^n \tilde{L}.$$

1014 ◀

1015 **Proof of Lemma 29.** Consider  $v(\tau^d) \subset K \cap \tau^d$ , where we use the definition (19) and choose  
 1016 an arbitrary  $n$  dimensional simplex  $\sigma^n \subset K \cap \tau^d$ . Note that  $v(\tau^d) \in K \cap \tau^d$ . Thanks to  
 1017 Lemma 27,

$$1018 \quad \sin \angle(\text{aff}(\sigma^n), T_v \mathcal{M}) \leq \frac{(\alpha_{d-n})^{4+n}}{6(n+1)} \zeta^n.$$

1019 From this bound we conclude that

$$1020 \quad d_H(T_v \mathcal{M} \cap B(v, 2L), \text{aff}(\sigma^n) \cap B(v, 2L)) \leq 2 \frac{(\alpha_{d-n})^{4+n}}{6(n+1)} \zeta^n L,$$

1021 where  $d_H$  denotes the Hausdorff distance. Because of Lemma 6 and (8), we have that

$$1022 \quad d_H(T_v \mathcal{M} \cap B(v, 2L), \pi_v^{-1}(B_{T_v \mathcal{M}}(v, 2L))) \leq \frac{(\alpha_{d-n})^{4+2n}}{6(n+1)^2} \zeta^{2n} L,$$

1023 where  $B_{T_v \mathcal{M}}(v, 2L)$  denotes the ball in  $T_v \mathcal{M}$  with radius  $2L$  and centre  $v$ . This gives us

$$\begin{aligned}
 1024 \quad d_H(\text{aff}(\sigma^n) \cap B(v, 2L), \pi_v^{-1}(B_{T_v \mathcal{M}}(v, 2L))) \\
 1025 \quad \leq 2 \frac{(\alpha_{d-n})^{4+n}}{6(n+1)} \zeta^n L + \frac{(\alpha_{d-n})^{4+2n}}{6(n+1)^2} \zeta^{2n} L \quad (\text{by the triangle inequality}) \\
 1026 \quad \leq \frac{(\alpha_{d-n})^{4+n} \zeta^n}{n+1} L.
 \end{aligned}$$

1027 Because  $\mathcal{M} \cap \tau \subset \pi_v^{-1}(B_{T_v \mathcal{M}}(v, 2L))$  and the distance between  $\mathcal{M} \cap \tau$  and  $\text{aff}(\sigma^n)$  is small  
 1028 compared to the size of the neighbourhood of  $K$  given in Lemma 28, that is

$$1029 \quad \frac{(\alpha_{d-n})^{4+n} \zeta^n}{n+1} L \leq \frac{\left(\frac{16}{10}\right)^2 (\alpha_{d-n})^4}{n+1} \zeta^n (\alpha_{d-n-1})^n \tilde{L}, \quad (38)$$

1030  $\mathcal{M} \cap \tau$  is contained in this neighbourhood of  $K$ . ◀